



## SPECTROSCOPIC CHARACTERIZATION AND CYTOTOXIC ACTIVITY OF NEW METAL COMPLEXES DERIVED FROM (1E, N'Z, N'Z)-N',N'-BIS(2-HYDROXYBENZYLIDENE)-2-(NAPHTHALEN-1-YLOXY) ACETOHYDRAZONOHYDRAZIDE.

A. S. El-Tabl<sup>1</sup>, M. M. Abd-El Wahed<sup>2</sup>, M. A. Wahba<sup>3</sup>  
and M. A. Shebl<sup>1</sup>

<sup>1</sup>Department of Chemistry, Faculty of Science, El-Menoufia University, Shebin El- Kom, Egypt.

<sup>2</sup>Department of Pathology, Faculty of Medicine, El-Menoufia University, Shebin El- Kom, Egypt.

<sup>3</sup>Department of Inorganic Chemistry, National Research Center, Dokki, Giza, Egypt.

**Abstract:** Spectroscopic (IR, <sup>1</sup>H-NMR, UV-visible, mass and ESR spectra) and structural studies of the ligand (1E, N'Z, N'Z)-N', N'-bis (2-hydroxybenzylidene)-2-(naphthalen-1-yloxy) acetohydrazonehydrazide (H<sub>2</sub>L) and its metal complexes are reported. The magnetic properties and thermal analyses (DTA and TGA) were also carried out. The IR spectra of the prepared complexes suggested that, the ligand adopted either a bidentate or a tetradentate fashion, bonding to the metal ion through the azomethine nitrogens and the two phenolic oxygen atoms (ONNO). Electronic spectra and magnetic susceptibility measurements revealed an octahedral geometry for all complexes except silver(I) complex (6), copper(II) complex (7) and cobalt(II) complex (11). The elemental analyses and mass spectral data have justified the ML, ML<sub>2</sub> and M<sub>3</sub>L composition of the complexes. The ESR spectra of copper(II) complexes (5), (7), (12) and (16), showed an axial type (dx<sup>2</sup>-y<sup>2</sup>) ground state with a covalent bond character and also support the suggested structures of complexes. The cytotoxicity of the ligand and its metal complexes were investigated and discussed.

**Indexing terms/Keywords:**-Cytotoxic activity; hydrazine complexes; spectral and magnetic studies.



## Council for Innovative Research

Peer Review Research Publishing System

**Journal:** Journal of Advances in Chemistry

Vol. 11, No. 9

[www.cirjac.com](http://www.cirjac.com)

[editorjaconline@gmail.com](mailto:editorjaconline@gmail.com), [editor@cirjac.com](mailto:editor@cirjac.com)



## 1. INTRODUCTION

New synthetic compounds with novel mechanism of action have become an important task to cope with drug resistance problems. Schiff bases have largely been recognized as useful building blocks in the synthesis of biologically important compounds [1-3]. Considerable studies have been reported regarding their biological activities as anticancer, antibacterial, antifungal, and herbicidal activities [4-8]. However, many organic drugs require interaction with metals in order to enhance their activity. They interact with metals at their target site or during their metabolism or disturb the balance of metal ion uptake and distribution in cells and tissues. Understanding these interactions helps a lot in synthesizing of influential metallo-pharmaceuticals and implementation of new co-therapies. Metal complexes have unique properties enhancing their bioactivity. An important property is the ability of metals to form positively charged ions in aqueous solutions that can bind to negatively charged biological molecules [9-12]. The high electron affinity of metal ions can significantly polarize groups that are coordinated to them, leading to the generation of hydrolysis reactions [10]. Furthermore, metal ions also has the ability to coordinate ligands in a three dimensional configuration, thus allowing functionalization of groups that can be tailored to defined molecular targets [13,14,7]. Much concern has been drawn toward hydrazine and their metal complexes due to their biological activities as fungicides [15,16], bactericides [17], analgesic and anti-inflammatory [18], antioxidant [19,20], antitumor [21-23] and insecticidal [24]. Literature survey on structural behavior of hydrazine complexes reveals some interesting features of its coordination behavior. As a ligand, hydrazine offers the possibility of different modes of coordination towards transition metal ions. It can function as a monodentate and or bridging bidentate ligand [2,25]. Reactions of hydrazines with complexes containing multiple bonds can give rise to complexes containing coordinated imido-, diazenido- and nitrido-ligands [26-28]. In view of the above facts, this article aimed to synthesize and identify new metal complexes derived from a hydrazine Schiff base ligand. The coordination behavior of the ligand towards metals ions has been investigated via variety of physicochemical techniques. The cytotoxic activity of the ligand as well as its metal complexes was tested against human colon cancer cells (HCT-116 cell line) and hepatocellular carcinoma (HEPG-2 cell line) comparing with standard drug Vinblastine. Furthermore, the antimicrobial activity of some metal complexes against *Aspergillus fumigates*, *Candida albicans*, *Streptococcus pneumonia*, *Bacillus subtilis*, *Pseudomonas aeruginosa* and *Escherichia coli* was also investigated.

## 2. EXPERIMENTAL

### 2.1. Materials

All reagents employed for the preparation of the ligand and its complexes were of the analytical grade available and used without further purification. Metal salts were provided from Sigma-Aldrich Company. 1-naphthol (Assay 99 %) and ethylchloroacetate (Assay 99 %), hydrazine hydrate (Assay  $\geq 99.99$  %), 2-hydroxy benzaldehyde (Assay  $\geq 98$  %), DMSO (Assay 99.7%) and absolute ethanol (Assay  $\geq 99.8$  %) were also obtained from Sigma-Aldrich Company.

### 2.2. Instrumentation and measurements

C, H, N and Cl were analysed at the Microanalytical center, Cairo University, Egypt. Standard analytical method (gravimetric) was used to determine the metal ion content [29-31]. FT-IR spectra of the ligand and its metal complexes were measured using KBr discs by a Jasco FT/IR 300E Fourier transform infrared spectrophotometer covering the range 400-4000  $\text{cm}^{-1}$ . Electronic spectra in the 200-900 nm regions were recorded on a Perkin-Elmer 550 spectrophotometer. The thermal analyses (DTA and TGA) was carried out on a Shimadzu DT-30 thermal analyzer from room temperature to 800°C at a heating rate of 10 °C/min. Magnetic susceptibilities were measured at 25°C by the Gouy method using mercuric tetrathiocyanatocobaltate(II) as the magnetic susceptibility standard. Diamagnetic corrections were estimated from Pascal's constant [32]. The magnetic moments were calculated from the equation:

$$\mu_{\text{eff.}} = 2.84 \sqrt{\chi_M^{\text{corr}} \cdot T}$$

The molar conductance of  $10^{-3}$  M solution of the complexes in DMSO was measured at 25°C with a Bibby conductometer type MCI. The resistance measured in ohms and the molar conductivities were calculated according to the equation:

$$\Lambda_M = V \cdot K \cdot g / M_w \cdot$$

Where: M = molar conductivity  $\text{l}^{-1}\text{cm}^2\text{mol}^{-1}$ , V = volume of the complex solution/ml, K = cell constant (0.92/  $\text{cm}^{-1}$ ),  $M_w$  = molecular weight of the complex, g = weight of the complex/g, =resistance/.  $^1\text{H-NMR}$  spectra were obtained on BRUKER 400 MHz spectrometers. Mass spectra were recorded using GC/MS Shimadzu 5050 QA mass spectrometer. Chemical shifts (ppm) are reported relative to TMS. ESR measurements of solid complexes at room temperature were made using a Varian E-109 spectrophotometer with DPPH as a standard material. TLC is used to confirm the purity of the compounds.

### 2.3. Synthesis of the ligand

The ligand [H<sub>2</sub>L] was prepared by a three-step reactions (Figure 1). The first one involved addition of equimolar amount of 1-naphthole (10 g, 1.0 mol), to ethylchloroacetate (7.38 ml, 0.1 mol) in the presence of KOH (4.5 g, 0.10 mol) in 50  $\text{cm}^3$  of absolute ethanol. The mixture was refluxed on water bath for 6 hours and the formed precipitate was filtered off, washed with water, dried and recrystallized from ethanol to afford ethyl (1-naphthoxy) acetate (I). The second step includes mixing equimolar amount of ethyl (1-naphthoxy) acetate (I) (6.5 g, 0.01 mol) with hydrazine hydrate (2.7 ml, 0.02 mol) in 50  $\text{cm}^3$  of absolute methanol. The solution was refluxed with stirring for 4 hours, and the formed yellow product was filtrated off, washed with water, and dried to give pure needle shaped crystals of 2-(naphthalene-1-yloxy) acetohydrazide

(II). The final step involved addition of an equimolar amount of 2-(naphthalene-1-yloxy) acetohydrazide (II) (5.0 g, 0.01 mol) to 2-hydroxy benzaldehyde (5.6 g, 0.01 mol) in 50 cm<sup>3</sup> of absolute methanol. The mixture was refluxed with continuous stirring for 3 hours. After cooling, the solvent was removed under reduced pressure to give the ligand [H<sub>2</sub>L], (1E, N'Z, N'Z)-N', N'-bis (2-hydroxybenzylidene)-2-(naphthalene-1-yloxy) acetohydrazono- hydrazide.

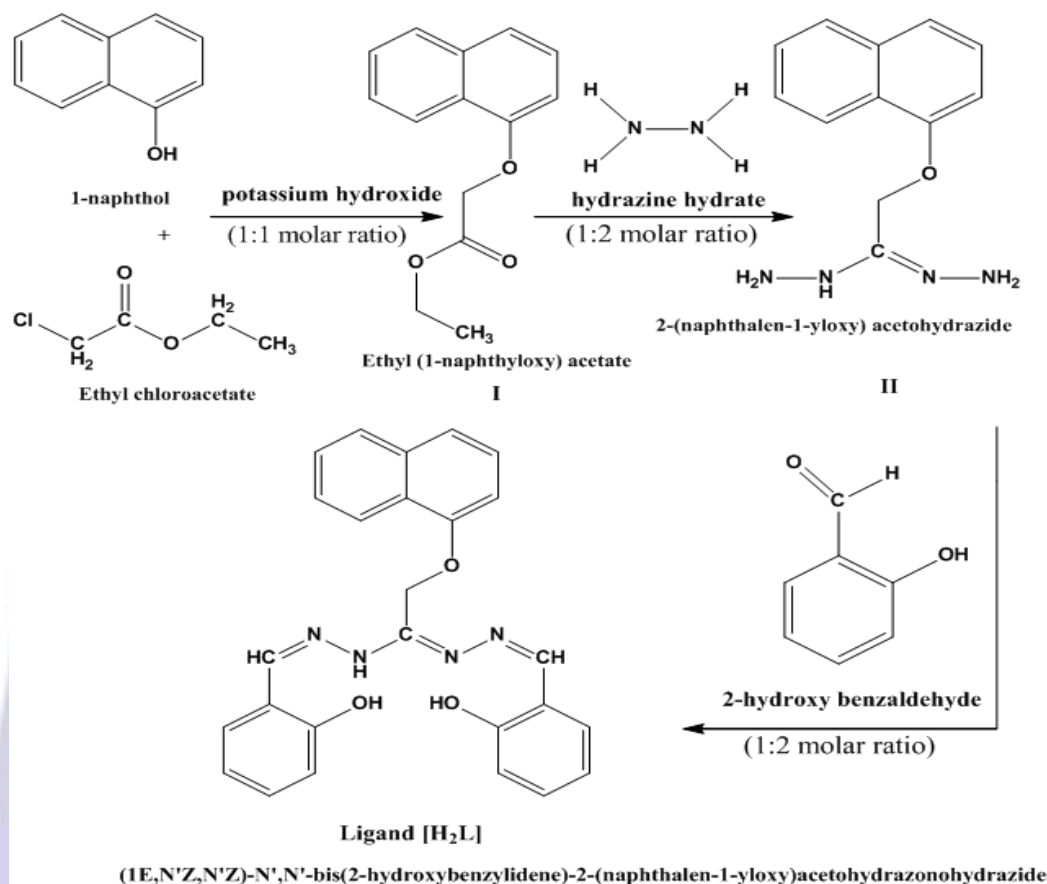


**Figure 1: Synthesis of the ligand [H<sub>2</sub>L]**

### 2.3.1. Preparation of complexes (2)-(19)

To the ligand (1) (1.0 g, 0.002 mol) in ethanol (50 cm<sup>3</sup>) was added ethanolic solution of (0.568 g, 0.002 mol) of Co(OAc)<sub>2</sub>·4H<sub>2</sub>O, (1L:1M), complex (2), (0.898g, 0.003 mol) of NiSO<sub>4</sub>·6H<sub>2</sub>O, (2L:3M), complex (3), to the ligand (1.0 g, 0.002 mol) in ethanol (50 cm<sup>3</sup>) was added (0.567 g, 0.002 mol) Ni(OAc)<sub>2</sub>·4H<sub>2</sub>O, (1L:1M), complex (4), to the ligand (1.0 g, 0.002 mol) in ethanol (50 cm<sup>3</sup>) was added (0.414 g, 0.002 mol) of Cu(OAc)<sub>2</sub>, (1L:1M), complex (5), (0.774 g, 0.004 mol) of Ag(NO<sub>3</sub>), (1L:2M), complex (6), (0.459g, 0.003 mol) of CuCl<sub>2</sub>, (2L:3M), complex (7), (0.951g, 0.003 mol) of FeSO<sub>4</sub>·7H<sub>2</sub>O, (2L:3M), complex (8), (0.432 g, 0.001 mol) of Pb(OAc)<sub>2</sub>, (2L:1M), complex (9), (0.279 g, 0.001 mol) of Mn(OAc)<sub>2</sub>·4H<sub>2</sub>O, (2L:1M), complex (10), (0.529g, 0.003 mol) of CoSO<sub>4</sub>, (2L:3M), complex (11), (0.551 g, 0.002) Cu(NO<sub>3</sub>)<sub>2</sub>·3H<sub>2</sub>O, (1L:1M), complex (12), (0.284 g, 0.001 mol) of Co(OAc)<sub>2</sub>·4H<sub>2</sub>O, (2L:1M), complex (13), (0.304 g, 0.001 mol) of Cd(OAc)<sub>2</sub>·2H<sub>2</sub>O, (2L:1M), complex (14), (0.500 g, 0.002 mol) of Zn(OAc)<sub>2</sub>·2H<sub>2</sub>O, (1L:1M), complex (15), (0.853g, 0.003 mol) of CuSO<sub>4</sub>·5H<sub>2</sub>O, (2L:3M), complex (16), (0.363 g, 0.001 mol) of Hg(OAc)<sub>2</sub>, (2L:1M), complex (17), (0.304 g, 0.001 mol) of Sr(Cl)<sub>2</sub>·6H<sub>2</sub>O, (2L:1M), complex (18), (0.435 gm, 0.001 mol) of Ti(C<sub>2</sub>H<sub>3</sub>O<sub>2</sub>)<sub>3</sub>, (2L:1M), complex (19). The mixture was refluxed with stirring for 2-3 hrs, depending on the nature of the metal ion and the anion. When the precipitate appeared, it was removed by filtration, washed with ethanol and dried in vacuo over p<sub>4</sub>O<sub>10</sub>. Analytical data are given in Table 1.

## 2.4. Biological activity

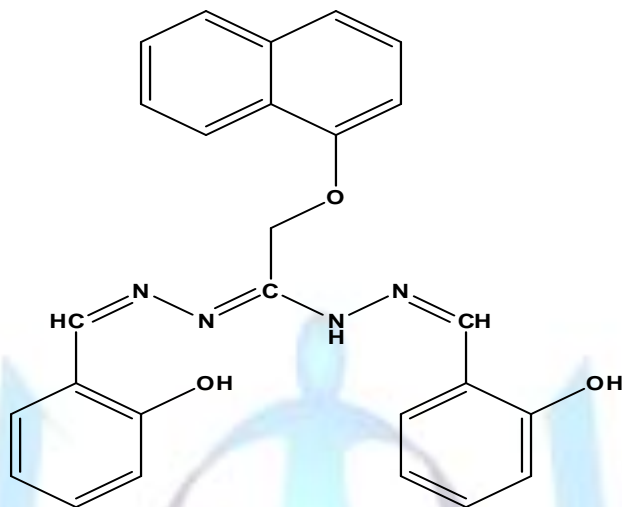
### 2.4.1. Cytotoxic activity

Evaluation of the cytotoxic activity of the ligand and its metal complexes was carried out in the Pathology Laboratory, Pathology Department, Faculty of Medicine, El-Menoufia University, Egypt. The evaluation process was carried out in vitro using the Sulfo-Rhodamine-B-stain (SRB) assay published method [33]. Cells were plated in 96-multiwell plate (10<sup>4</sup> cells/well) for 24 hrs. before treatment with the complexes to allow attachment of cell to the wall of the plate. Different concentrations of the compounds under test in DMSO (0, 5, 12.5, 25 and 50 µg/ml) were added to the cell monolayer, triplicate wells being prepared for each individual dose. Monolayer cells were incubated with the complexes for 48 hrs at 37°C and under 5% CO<sub>2</sub>. After 48 hrs. cells were fixed, washed and stained with Sulfo-Rhodamine-B-stain. Excess stain was wash with acetic acid and attached stain was recovered with Tris EDTA buffer. Color intensity was measured in an ELISA reader. The relation between surviving fraction and drug concentration is plotted to get the survival curve for each tumor cell line after addition the specified compound.

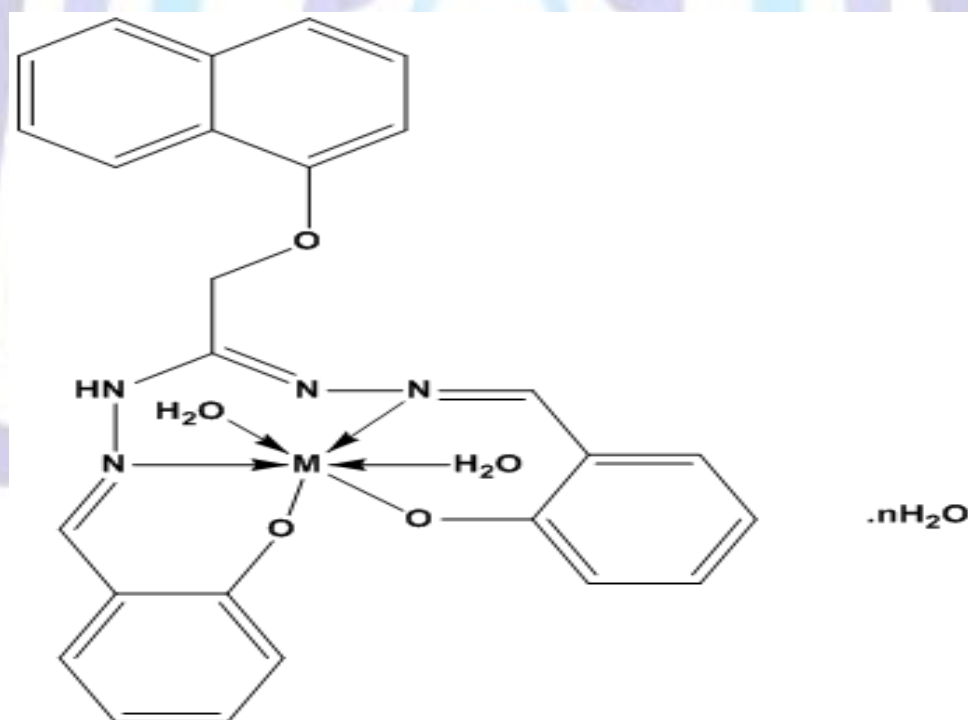


### 3. Results and discussion

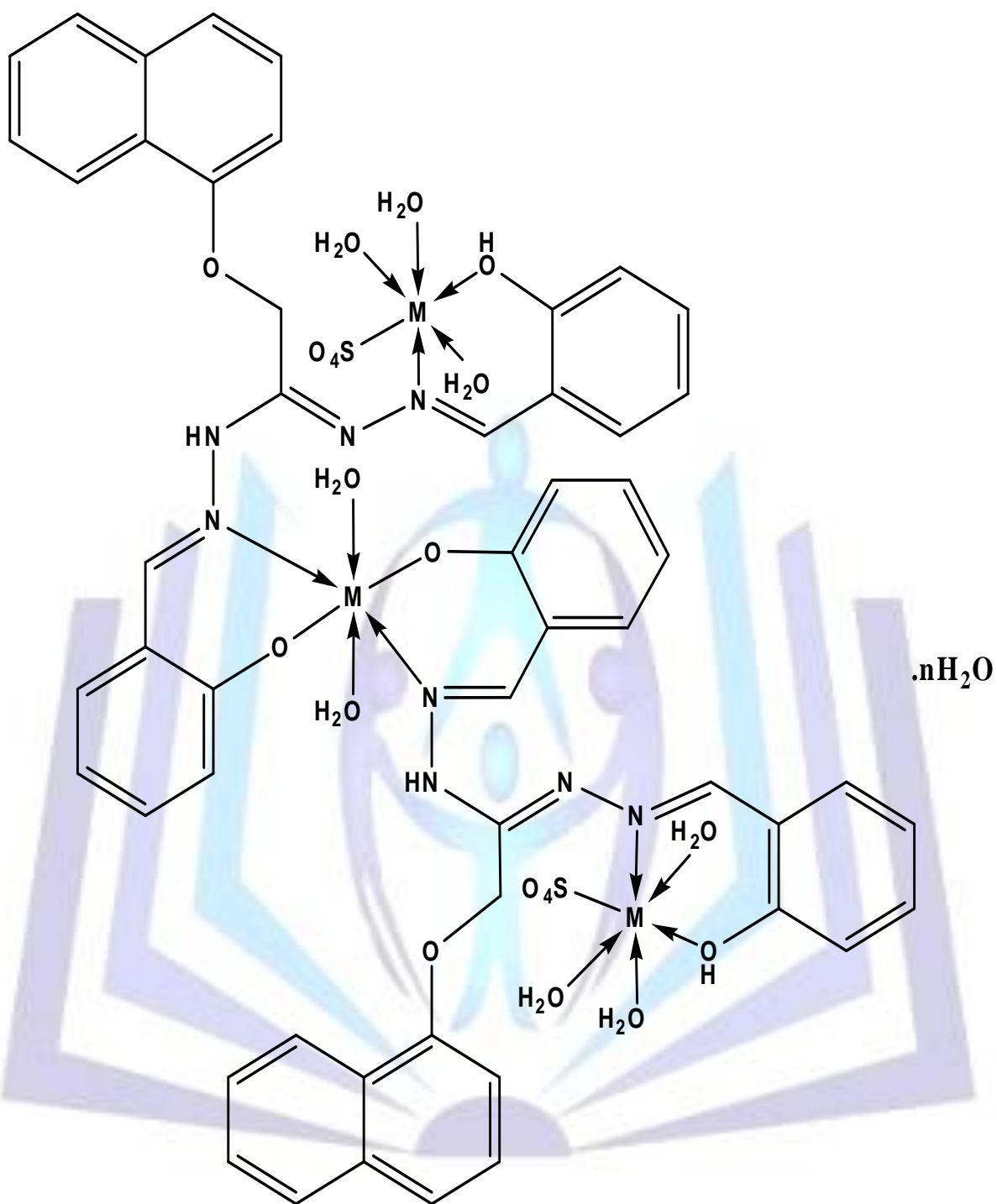
The complexes are colored, stable in air; they are soluble in polar solvents such as DMF and DMSO whereas they are insoluble in H<sub>2</sub>O, ethanol, CHCl<sub>3</sub> and benzene. All the complexes are non-electrolytes. The elemental analyses, spectral data [Tables 1-5] and thermal analyses [Table 6] are compatible with the proposed structures [Figure 2]. Many attempts were made to grow diffractable crystals, but unfortunately no crystal has been obtained until now.



**(1*E*,*N'**Z*,*N'**Z*)-*N*',*N'*-bis(2-hydroxybenzylidene)-2-(naphthalen-1-yloxy)acetohydrazonehydrazide Ligand**

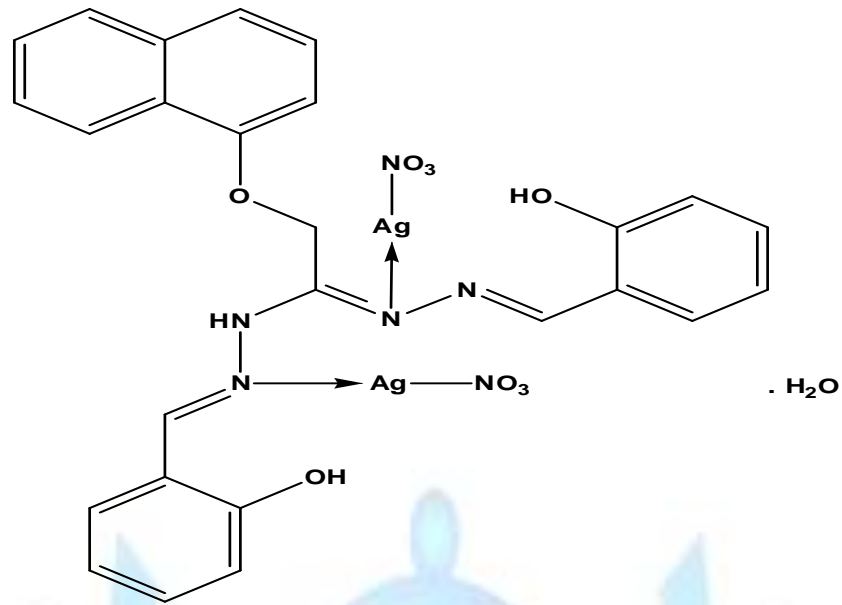


<b>Complex (2)</b>	<b>M= Co</b>	<b>n=1</b>
<b>Complex (4)</b>	<b>M=Ni</b>	<b>n=2</b>
<b>Complex (5)</b>	<b>M=Cu</b>	<b>n=2</b>

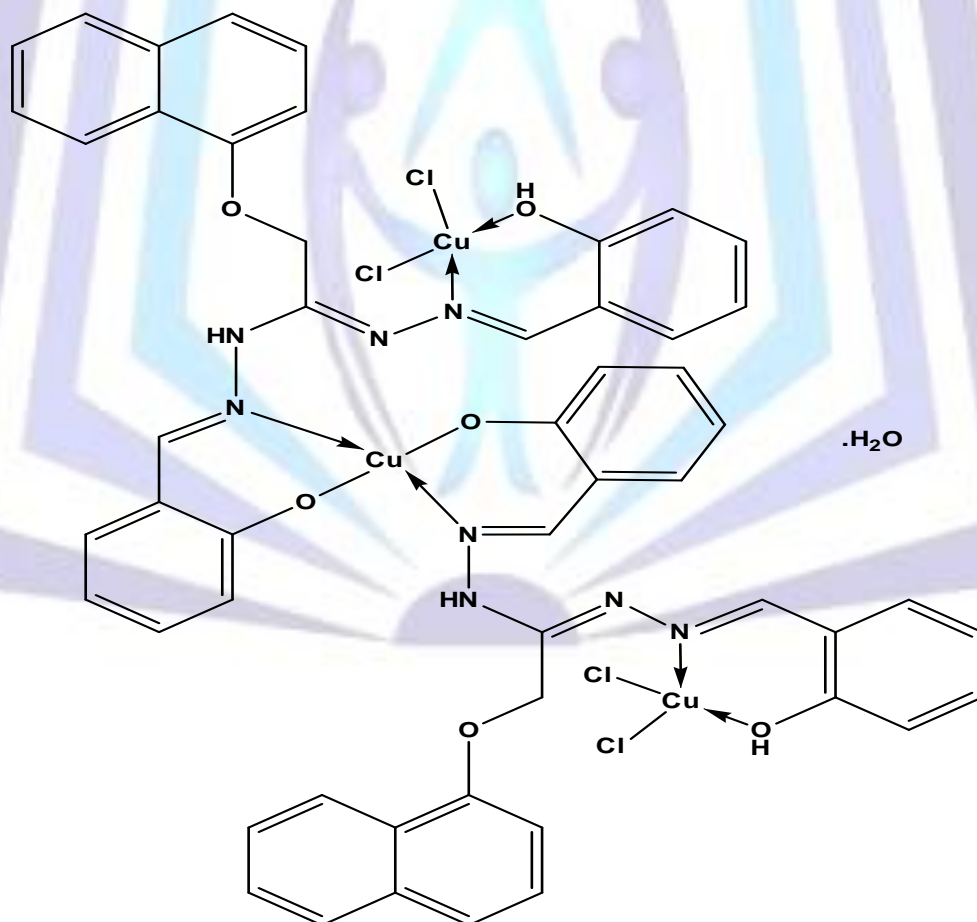


**Complex (3)**    M= Ni    n=2

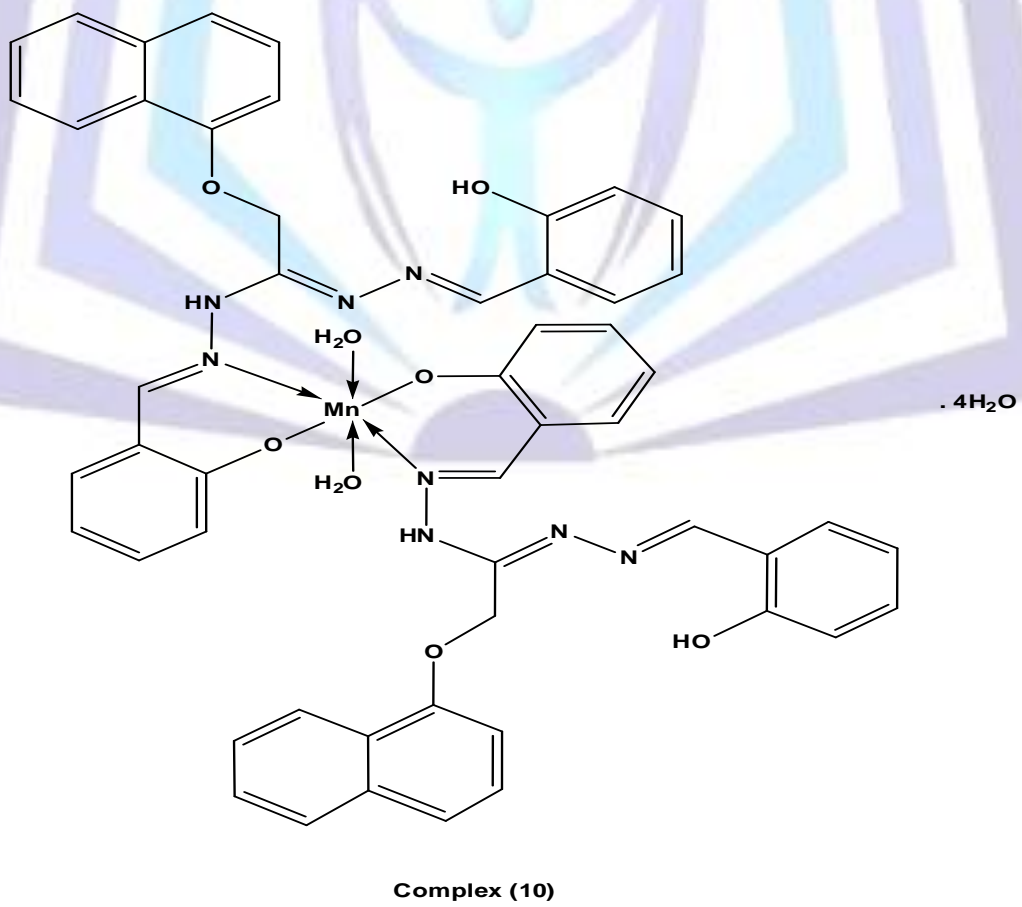
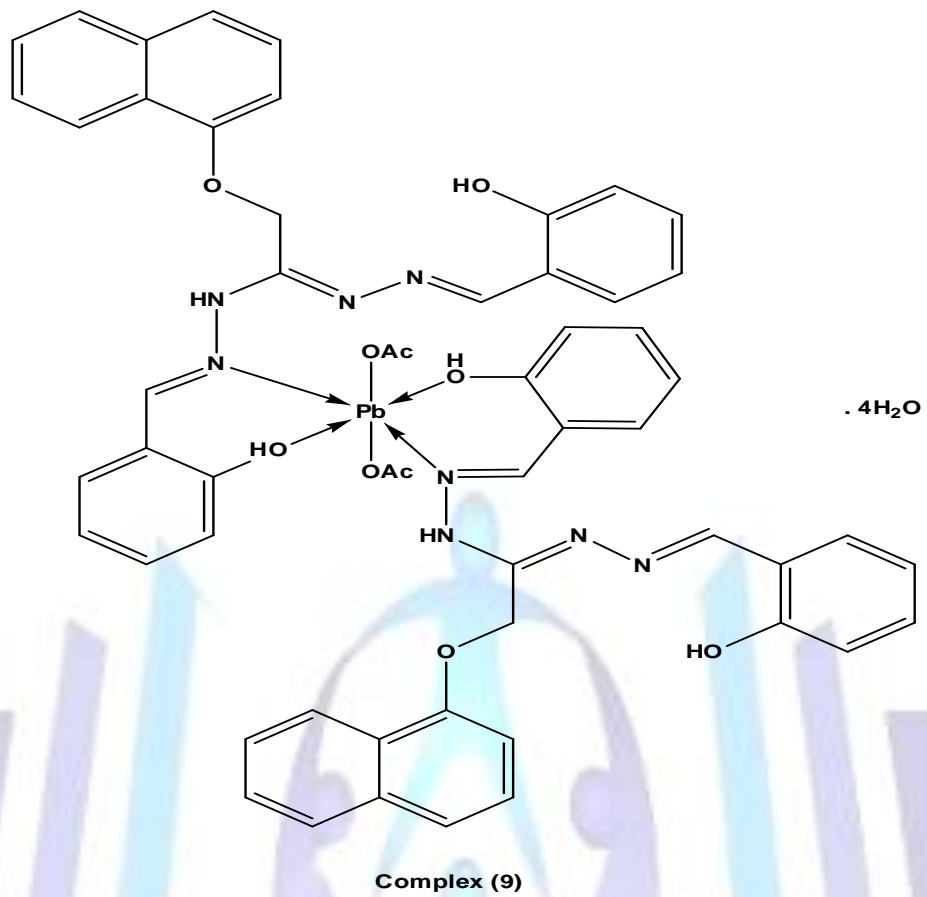
**Complex (8)**    M= Fe    n=1

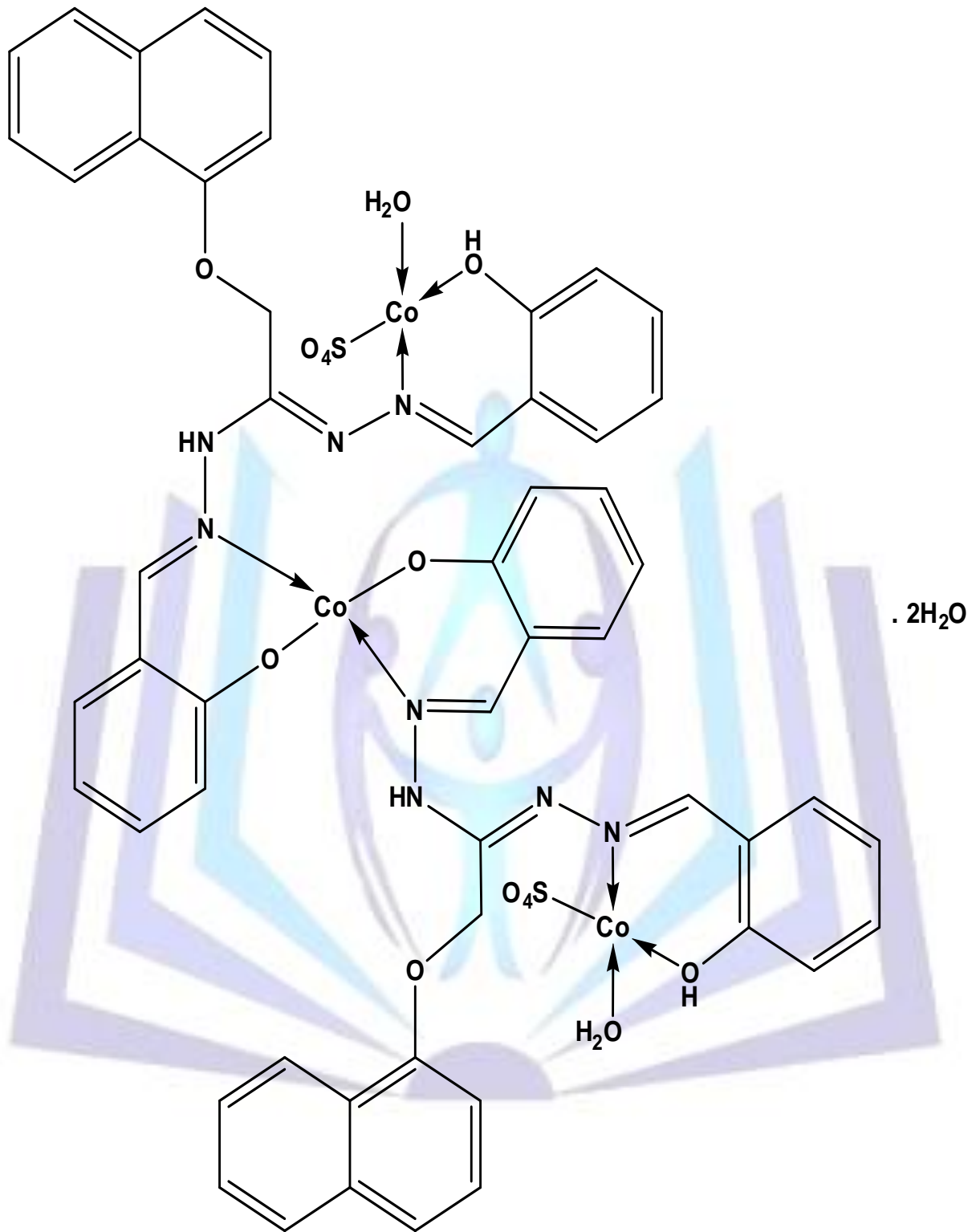


Complex (6)



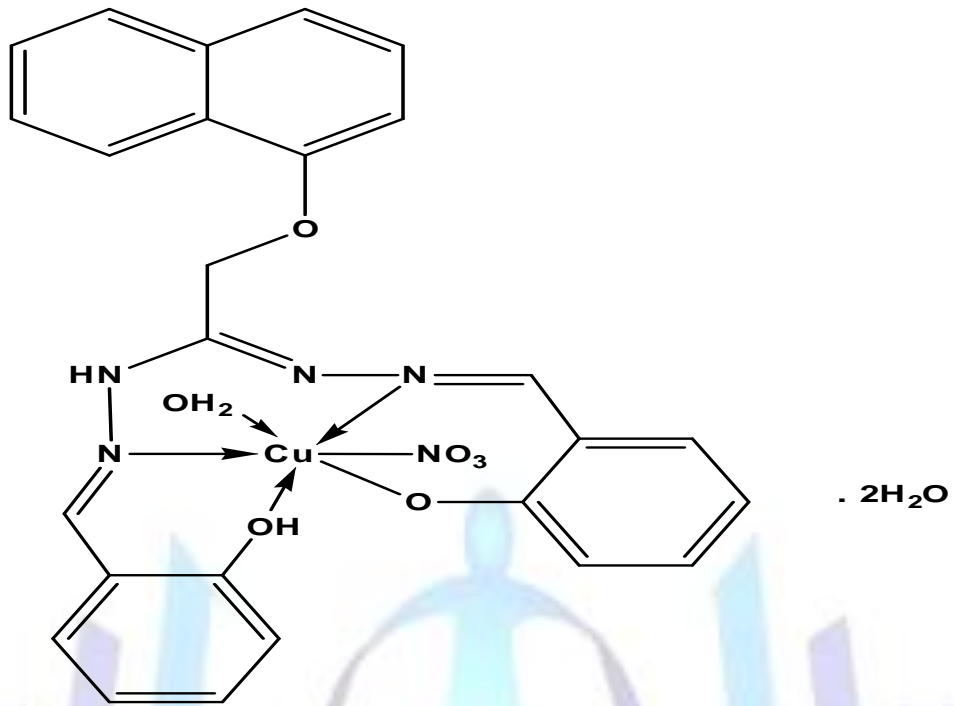
Complex (7)



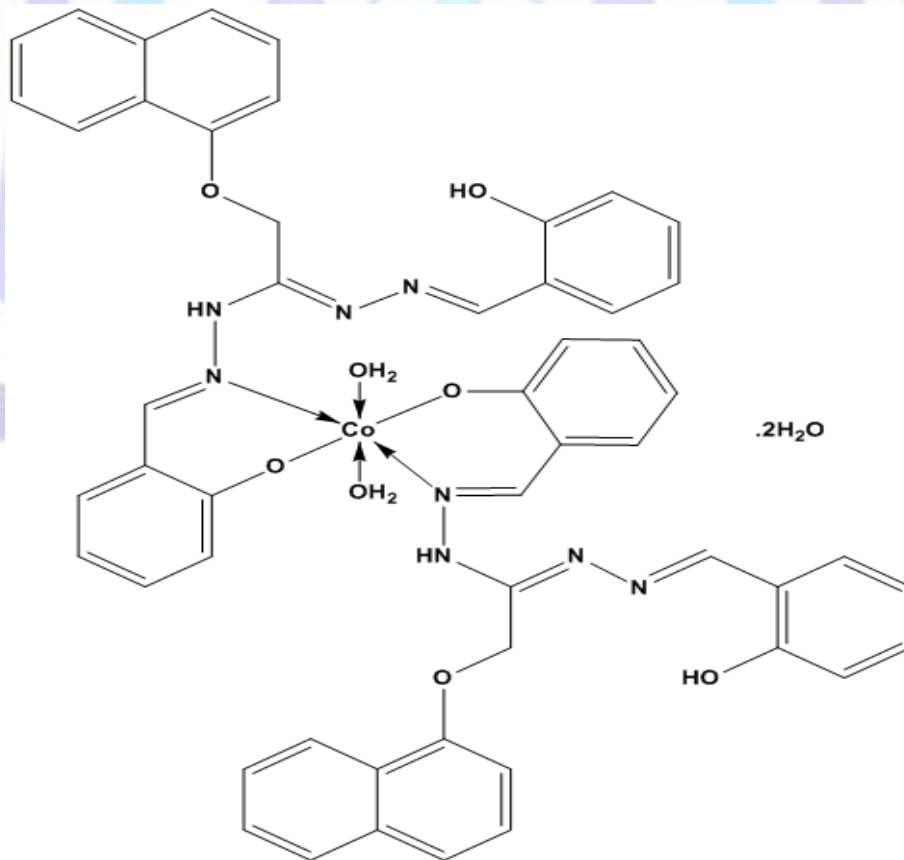


Complex (11)

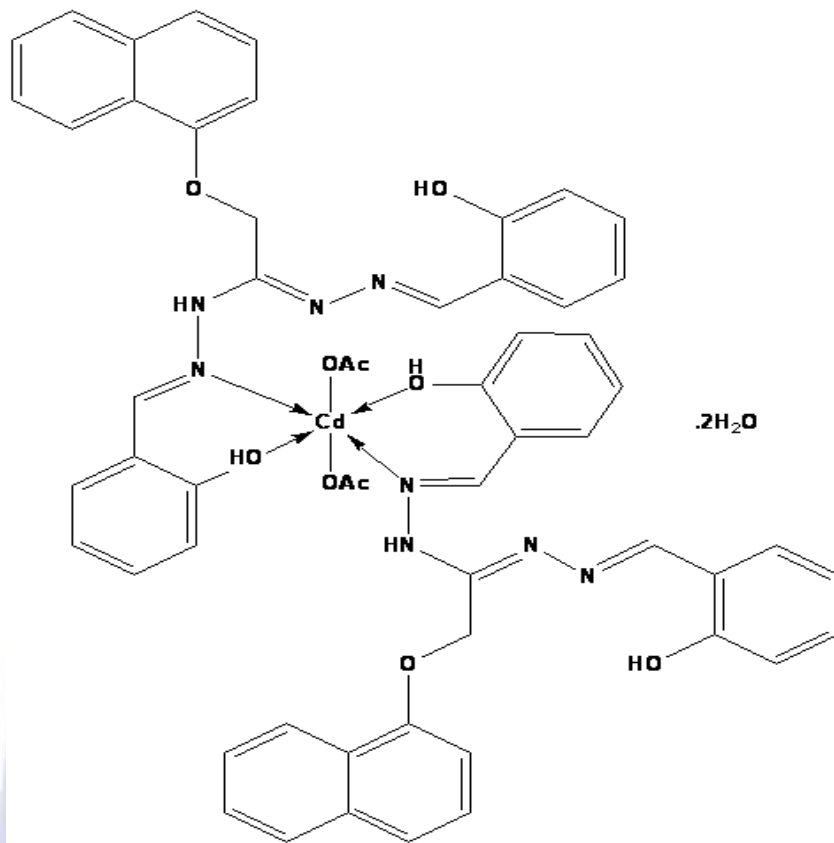




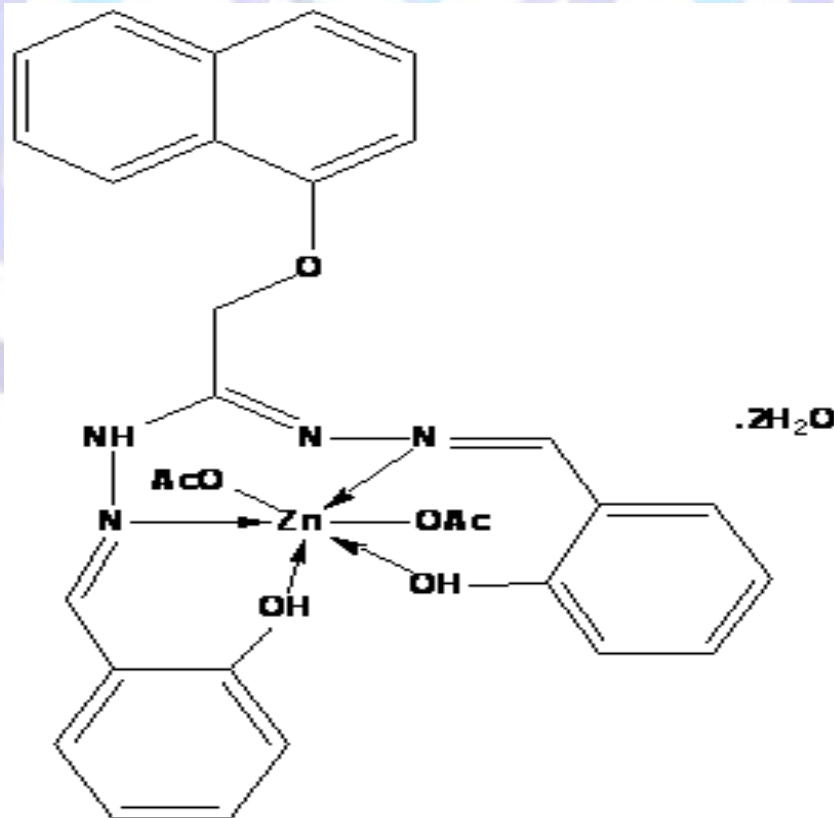
**Complex (12)**



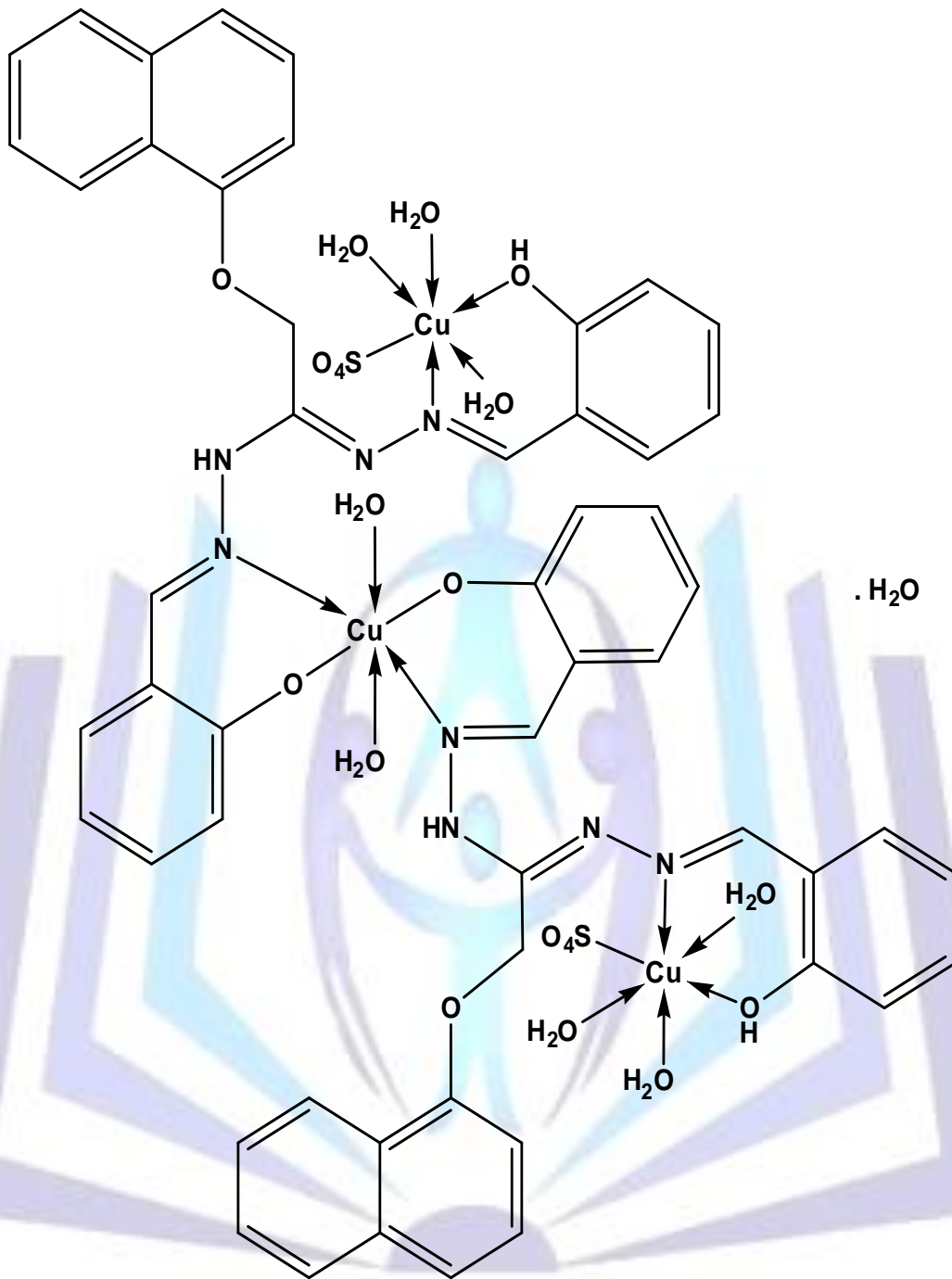
**Complex (13)**



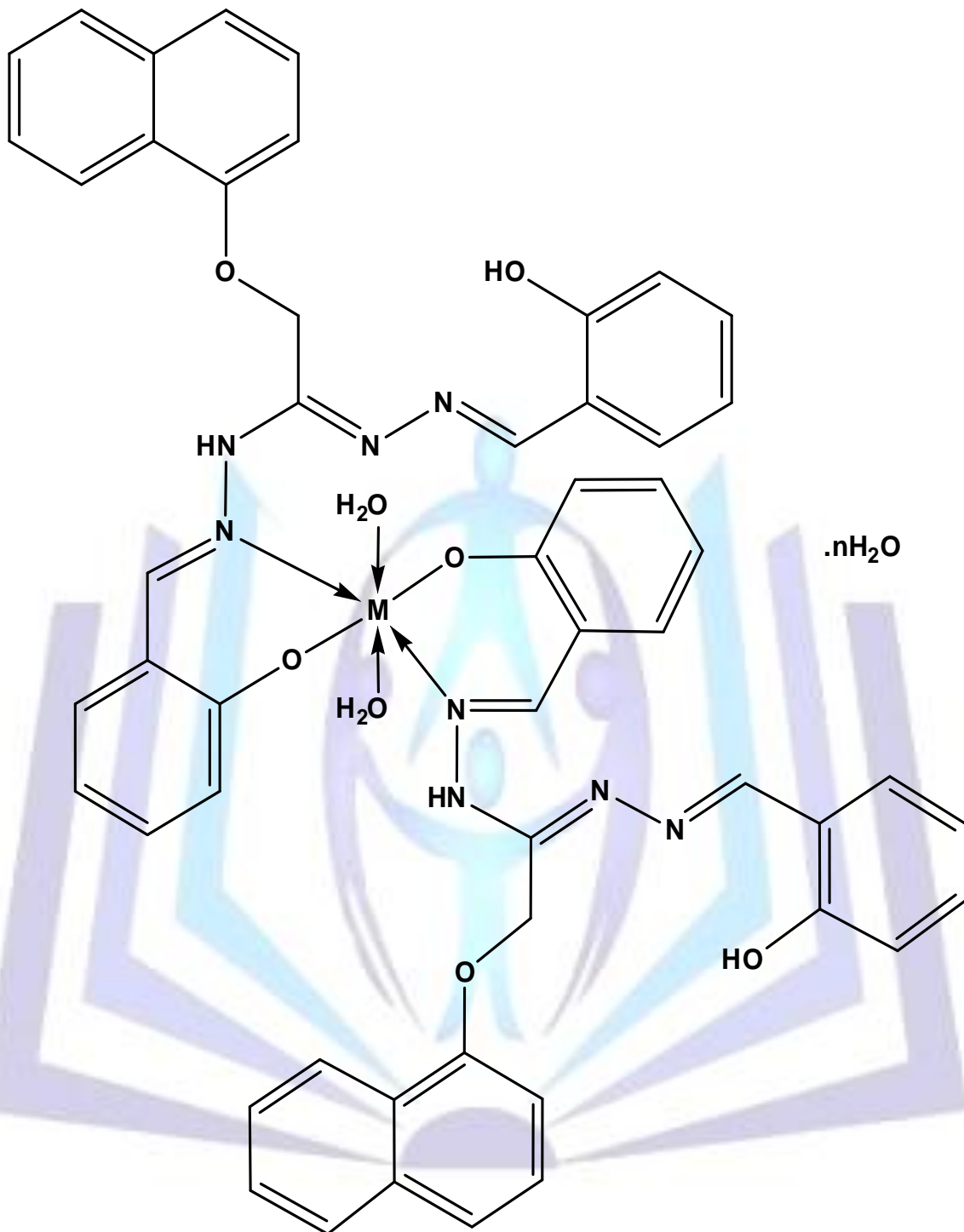
Complex (14)



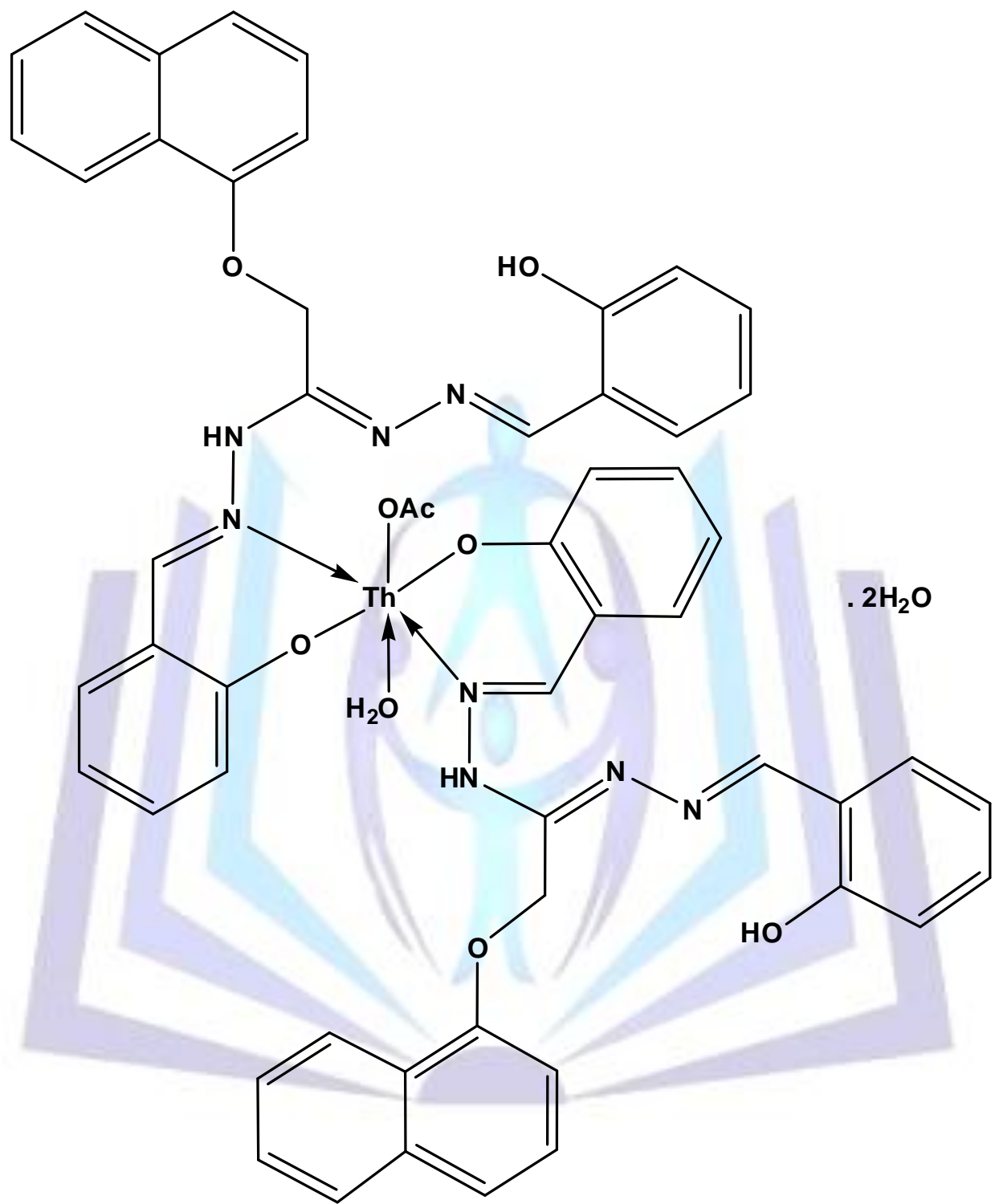
Complex (15)



Complex (16)



Complex (17) M=Hg n=1  
Complex (18) M=Sr n=4



**Complex (19)**

Figure 2. Proposed structures of the ligand [H<sub>2</sub>L] and its metal complexes (2)-(19)


 Table 1:-Analytical and Physical Data of the Ligand [H<sub>2</sub>L] (1) and its Metal Complexes.

No.	Ligands/Complexes	Color	FW	M.P (°C)	Yield (%)	Anal. /Found (Calc.) (%)					Molar conductance*
						C	H	N	M	Cl	
(1)	[H <sub>2</sub> L] C <sub>26</sub> H <sub>22</sub> N <sub>4</sub> O <sub>3</sub>	Beige	438.48	195	75	71.87(71.22)	4.71(5.06)	12.23(12.78)	–	–	–
(2)	[(L)Co(H <sub>2</sub> O) <sub>2</sub> ].H <sub>2</sub> O C <sub>26</sub> H <sub>26</sub> Co N <sub>4</sub> O <sub>6</sub>	Orange	549.44	>300	80	56.67(56.84)	4.75(4.77)	10.371(10.20)	10.61(10.73)	–	6.5
(3)	[(HL) <sub>2</sub> (Ni) <sub>3</sub> (SO <sub>4</sub> ) <sub>2</sub> (H <sub>2</sub> O) <sub>8</sub> ].2H <sub>2</sub> O C <sub>52</sub> H <sub>62</sub> N <sub>8</sub> Ni <sub>3</sub> O <sub>24</sub> S <sub>2</sub>	Beige	1423.30	>300	84	44.18(43.88)	4.0(4.39)	7.9(7.87)	12.23(12.37)	–	14.8
(4)	[(L)Ni(H <sub>2</sub> O) <sub>2</sub> ].2H <sub>2</sub> O C <sub>26</sub> H <sub>28</sub> N <sub>4</sub> Ni O <sub>7</sub>	Olive	567.22	>300	69	55.18(55.05)	4.98(4.98)	9.248(9.88)	10.11(10.35)	–	6.3
(5)	[(L)Cu(H <sub>2</sub> O) <sub>2</sub> ].2H <sub>2</sub> O C <sub>26</sub> H <sub>28</sub> Cu N <sub>4</sub> O <sub>7</sub>	Dark green	572.07	>300	71	54.24(54.59)	4.49(4.93)	9.86(9.79)	10.8(11.11)	–	13.2
(6)	[(H <sub>2</sub> L)(Ag) <sub>2</sub> (NO <sub>3</sub> ) <sub>2</sub> ].H <sub>2</sub> O C <sub>26</sub> H <sub>24</sub> Ag <sub>2</sub> N <sub>6</sub> O <sub>10</sub>	Beige	796.24	236	80	38.9(39.22)	2.98(3.04)	10.33(10.55)	26.8(27.09)	–	7.85
(7)	[(HL) <sub>2</sub> (Cu) <sub>3</sub> (Cl) <sub>4</sub> ].H <sub>2</sub> O C <sub>52</sub> H <sub>44</sub> Cl <sub>4</sub> Cu <sub>3</sub> N <sub>8</sub> O <sub>7</sub>	Beige	1225.41	210	72	50.81(50.97)	3.98(3.62)	9.0(9.14)	15.1(15.56)	11.4(11.57)	17.3
(8)	[(HL) <sub>2</sub> (Fe) <sub>3</sub> (SO <sub>4</sub> ) <sub>2</sub> (H <sub>2</sub> O) <sub>8</sub> ].H <sub>2</sub> O C <sub>52</sub> H <sub>60</sub> Fe <sub>3</sub> N <sub>8</sub> O <sub>23</sub> S <sub>2</sub>	Olive	1396.74	242	68	44.40(44.72)	4.1(4.33)	7.9(8.02)	11.33(11.99)	–	16.4
(9)	[(HL) <sub>2</sub> Pb(OAc) <sub>2</sub> ].4H <sub>2</sub> O C <sub>56</sub> H <sub>58</sub> N <sub>8</sub> O <sub>14</sub> Pb	Grey	1274.30	223	65	52.38(52.78)	4.22(4.59)	8.65(8.79)	16.1(16.26)	–	11.3
(10)	[(HL) <sub>2</sub> Mn (H <sub>2</sub> O) <sub>2</sub> ].4H <sub>2</sub> O C <sub>52</sub> H <sub>54</sub> Mn N <sub>8</sub> O <sub>12</sub>	Brown	1037.97	238	65	59.80(60.17)	5.1(5.24)	10.6(10.80)	4.78(5.29)	–	7.5
(11)	[(HL) <sub>2</sub> (Co) <sub>3</sub> (SO <sub>4</sub> ) <sub>2</sub> (H <sub>2</sub> O) <sub>2</sub> ].2H <sub>2</sub> O C <sub>52</sub> H <sub>50</sub> Co <sub>3</sub> N <sub>8</sub> O <sub>18</sub> S <sub>2</sub>	Beige	1315.93	234	89	47.20(47.46)	3.5(3.83)	8.3(8.52)	13.0(13.44)	–	13.8
(12)	[(HL)Cu(NO <sub>3</sub> ) (H <sub>2</sub> O)].2H <sub>2</sub> O C <sub>26</sub> H <sub>27</sub> Cu N <sub>5</sub> O <sub>9</sub>	Brown	617.07	230	55	50.55(50.61)	4.37(4.41)	11.34(11.35)	10.29(10.30)	–	6.8
(13)	[(HL) <sub>2</sub> Co(H <sub>2</sub> O)].2H <sub>2</sub> O	Beige	1005.93	220	82	62.24(62.09)	4.62(5.01)	11.77(11.14)	6.19(5.86)	–	15.6



	$C_{52}H_{50}CoN_8O_{10}$										
(14)	$[(HL)_2Cd(OAc)_2] \cdot 2H_2O$ $C_{56}H_{54}CdN_8O_{12}$	Yellow	1143.49	>300	70	58.91(58.82)	4.14(4.76)	9.99(9.80)	9.73(9.83)	-	11.2
(15)	$[(H_2L)Zn(OAc)_2] \cdot 2H_2O$ $C_{30}H_{32}N_4O_9Zn$	Yellow	657.98	223	74	54.34(54.76)	4.01(4.90)	8.03(8.52)	9.8(9.94)	-	12.1
(16)	$[(HL)_2(Cu)_3(SO_4)_2(H_2O)_8] \cdot H_2O$ $C_{52}H_{60}Cu_3N_8O_{23}S_2$	Silver	1419.84	216	66	43.79(43.99)	4.16(4.26)	7.12(7.89)	12.98(13.43)	-	13.7
(17)	$[(HL)_2Hg(H_2O)_2] \cdot H_2O$ $C_{52}H_{48}HgN_8O_9$	Beige	1129.58	230	73	54.8(55.29)	4.0(4.28)	9.7(9.92)	17.3(17.76)	-	6.8
(18)	$[(HL)_2Sr(H_2O)_2] \cdot 4H_2O$ $C_{52}H_{54}N_8O_{12}Sr$	Beige	1070.65	240	76	58.1(58.33)	4.8(5.08)	10.2(10.47)	7.89(8.18)	-	7.2
(19)	$[(HL)_2Th(OAc)(H_2O)] \cdot 2H_2O$ $C_{54}H_{51}N_8O_{11}Th$	Beige	1220.07	245	60	52.89(53.16)	4.1(4.21)	8.9(9.18)	18.77(19.02)	-	8.3

\*  $M^{-1} cm^2 mol^{-1}$

Table 2:- IR Frequencies of the Bands ( $cm^{-1}$ ) of Ligand [H<sub>2</sub>L], (1) and its Metal Complexes

No.	$\nu(H_2O)$	$\nu(OH)$	$\nu(H-bonding)$	$\nu(NH)$	$\nu(N-N)$	$\nu(C=N)$	$\nu(COH/CO)$	$\nu(Ar)$	$\nu(OAc/SO_4/NO_3)$	$\nu(M-O)$	$\nu(M-N)$	$\nu(M-Cl)$
(1)	-	3465, 3446	3650-3310 3280-2650	3220	1031	1623, 1618	1316	1573,784 1550,752	-	-	-	-
(2)	3550-3480	-	3620-3280 3270-2850	3230	1040	1615, 1605	1301	1541,791 1471,757	-	587	453	-
(3)	3550-3490	3430	3610-3330 3320-2650	3238, 3225	1039	1623, 1618, 1610	1316, 1305	1571,783 1535,751	1157,1147, 730,682	618	565	-
(4)	3550-3480	-	3650-3210 3200-2670	3220	1037	1619, 1600	1309	1560,784 1550,754	-	587	545	-
(5)	3530-3485	-	3620-3280 3270-2680	3241	1035	1614, 1605	1305	1536,756	-	590	468	-
(6)	3650-3540	3466, 3447	3620-3320	3225	1037	1624, 1622	1316	1572-752	1330,1148	565	450	-



			3300-2650						890,752			-
(7)	3520-3475	3432	3602-3310 3300-2720	3223	1038	1619, 1610	1316, 1308	1572,748	-	575	465	415
(8)	3510-3470	3446	3580-3210 3200-2750	3231	1037	1623, 1618	1316, 1307	1517,751	1197,1157, 1147 682	617	565	-
(9)	3520-3465	3453, 3435	3570-3280 3270-2760	3217	1037	1624, 1616	1316	1572,784	1447,1330	565	459	-
(10)	3530-3450	3445	3610-3330 3320-2850	3322	1039	1624,1618	1316, 1307	1572,752	1455,1330	565	459	-
(11)	3500-3465	3430	3580-3280 3270-2680	3231	1036	1622	1315, 1309	1572,750	1195,1156, 1140 681,458	618	564	-
(12)	3560-3350	3456	3600-3210 3200-2680	3225	1039	1623, 1618	1316, 1307	1533,752	1327,1128 894,785	592	565	-
(13)	3565-3470	3445	3610-3315 3310-2650	3222	1037	1624,1618	1308	1572,783	-	546	550	-
(14)	3500-3480	3451, 3446	3600-3320 3310-2750	3226	1037	1624, 1620	1317	1572,752	1435,1335	565	460	-
(15)	3560	3455, 3431	3600-3300 3290-2650	3235	1038	1624, 1619	1315	1571,752	1471,1341	605	550	-
(16)	3550-3470	3437	3580-3280 3270-2680	3232	1037	1625, 1620	1316, 1308	1572,752	1206,1156, 1147 682,458	618	565	-
(17)	3520-3465	3435	3600-3260 3250-2630	3220	1037	1624, 1618	1316, 1308	1572,751	-	600	550	-
(18)	3520	3435	3580-3300 3290-2650	3222	1037	1625, 1620	1316, 1307	1572,751	-	580	520	-
(19)	3510	3437	3580-3285 3275-2700	3325	1037	1624, 1620	1316, 1307	1571,752	1446,1330	565	465	-





### 3.1. Conductivity measurements

The molar conductivity of  $110^{-3}$  M solution of the metal complexes (2-19) in DMSO at room temperature are given in experimental section. The value of molar conductance of all complexes is in the  $6.3-16.4 \text{ cm}^2\text{mol}^{-1}$  range indicating a non-electrolytic nature of these complexes confirming the involvement of the acetate, sulfate, nitrate and chloride anions in the coordination sphere.

### 3.2. Mass spectra

The mass spectrum of the ligand (1) revealed a molecular ion peak (m/z) at 438 a.m.u which is coincident with the formula weight of the ligand and supports the identity of the Structure. Furthermore, the fragments observed at m/z = 30, 43, 72, 77, 86, 91, 107, 117, 133, 147, 194, 206, 236, 284, 326, 398 and 438 corresponding to  $\text{C}_2\text{H}_6$ ,  $\text{C}_3\text{H}_7$ ,  $\text{C}_5\text{H}_{12}$ ,  $\text{C}_6\text{H}_5$ ,  $\text{C}_7\text{H}_2$ ,  $\text{C}_7\text{H}_7$ ,  $\text{C}_8\text{H}_{11}$ ,  $\text{C}_8\text{H}_5\text{O}$ ,  $\text{C}_8\text{H}_5\text{O}_2$ ,  $\text{C}_9\text{H}_7\text{O}_2$ ,  $\text{C}_{14}\text{H}_{12}\text{N}$ ,  $\text{C}_{15}\text{H}_{12}\text{N}$ ,  $\text{C}_{16}\text{H}_{14}\text{NO}$ ,  $\text{C}_{20}\text{H}_{14}\text{NO}$ ,  $\text{C}_{22}\text{H}_{16}\text{NO}_2$ ,  $\text{C}_{24}\text{H}_{22}\text{N}_4\text{O}_2$  and  $\text{C}_{26}\text{H}_{22}\text{N}_4\text{O}_3$  moieties respectively. However, the spectrum of Cu(II) complex (5) spectrum shows a peak (m/z) at 571 a.m.u corresponding to the formula weight of the complex. Additionally, the peaks observed at 30, 41, 57, 63, 81, 98, 118, 180, 198, 228, 250, 279, 322, 337, 365, 393, 412, 438, 517 and 571 are due to  $\text{C}_2\text{H}_6$ ,  $\text{C}_3\text{H}_5$ ,  $\text{C}_4\text{H}_9$ ,  $\text{C}_3\text{H}_{11}\text{O}$ ,  $\text{C}_4\text{H}_{17}\text{O}$ ,  $\text{C}_5\text{H}_8\text{NO}$ ,  $\text{C}_5\text{H}_8\text{NO}$ ,  $\text{C}_6\text{H}_{16}\text{NO}$ ,  $\text{C}_9\text{H}_{12}\text{N}_2\text{O}_2$ ,  $\text{C}_{10}\text{H}_{18}\text{N}_2\text{O}_2$ ,  $\text{C}_{11}\text{H}_{20}\text{N}_2\text{O}_3$ ,  $\text{C}_{14}\text{H}_{22}\text{N}_2\text{O}_2$ ,  $\text{C}_{16}\text{H}_{11}\text{N}_2\text{O}_3$ ,  $\text{C}_{19}\text{H}_{18}\text{N}_2\text{O}_3$ ,  $\text{C}_{20}\text{H}_{21}\text{N}_2\text{O}_3$ ,  $\text{C}_{20}\text{H}_{19}\text{N}_3\text{O}_4$ ,  $\text{C}_{21}\text{H}_{19}\text{N}_3\text{O}_5$ ,  $\text{C}_{21}\text{H}_{19}\text{CuNO}_4$ ,  $\text{C}_{22}\text{H}_{19}\text{CuN}_2\text{O}_4$ ,  $\text{C}_{24}\text{H}_{28}\text{CuN}_3\text{O}_6$  and  $\text{C}_{26}\text{H}_{28}\text{CuN}_4\text{O}_7$  moieties respectively. The spectrum of Zn(II) complex (15) spectrum shows a peak (m/z) at 657 a.m.u corresponding to the formula weight of the complex. Additionally, the peaks observed at 18, 28, 44, 65, 77, 93, 109, 141, 169, 195, 212, 226, 251, 265, 304, 321, 337, 359, 395, 413, 448, 547, 577, 607, 639 and 657 are due to  $\text{CH}_6$ ,  $\text{C}_2\text{H}_4$ ,  $\text{C}_3\text{H}_8$ ,  $\text{C}_5\text{H}_5$ ,  $\text{C}_6\text{H}_5$ ,  $\text{C}_7\text{H}_9$ ,  $\text{C}_8\text{H}_{13}$ ,  $\text{C}_9\text{H}_{17}\text{O}$ ,  $\text{C}_{10}\text{H}_{17}\text{O}_2$ ,  $\text{C}_{12}\text{H}_{19}\text{O}_2$ ,  $\text{C}_{12}\text{H}_{20}\text{O}_3$ ,  $\text{C}_{12}\text{H}_{20}\text{NO}_3$ ,  $\text{C}_{14}\text{H}_{21}\text{NO}_3$ ,  $\text{C}_{14}\text{H}_{21}\text{N}_2\text{O}_3$ ,  $\text{C}_{17}\text{H}_{24}\text{N}_2\text{O}_3$ ,  $\text{C}_{17}\text{H}_{25}\text{N}_2\text{O}_4$ ,  $\text{C}_{17}\text{H}_{25}\text{N}_2\text{O}_5$ ,  $\text{C}_{25}\text{H}_{15}\text{N}_2\text{O}$ ,  $\text{C}_{28}\text{H}_{15}\text{N}_2\text{O}$ ,  $\text{C}_{28}\text{H}_{17}\text{N}_2\text{O}_2$ ,  $\text{C}_{28}\text{H}_{20}\text{N}_2\text{O}_4$ ,  $\text{C}_{28}\text{H}_{24}\text{N}_3\text{O}_5\text{Zn}$ ,  $\text{C}_{29}\text{H}_{26}\text{N}_3\text{O}_6\text{Zn}$ ,  $\text{C}_{30}\text{H}_{28}\text{N}_3\text{O}_7\text{Zn}$ ,  $\text{C}_{30}\text{H}_{28}\text{N}_4\text{O}_8\text{Zn}$  and  $\text{C}_{30}\text{H}_{30}\text{N}_4\text{O}_9\text{Zn}$  moieties respectively. The fragments of the ligand (1), Cu(II) complex (5) and Zn(II) complex (15) are represented in Table 3.

Table 3: Mass spectra of [H<sub>2</sub>L] (1), Cu(II) complex (5) and Zn(II) complex (15) i. Mass spectrum of the ligand [H<sub>2</sub>L]

m/z	Rel. Int.	Assignments
30	49	(C <sub>2</sub> H <sub>6</sub> )
43	14	(C <sub>3</sub> H <sub>7</sub> )
72	37	(C <sub>5</sub> H <sub>12</sub> )
77	6	(C <sub>6</sub> H <sub>5</sub> )
86	8	(C <sub>7</sub> H <sub>2</sub> )
91	13	(C <sub>7</sub> H <sub>7</sub> )
107	25	(C <sub>8</sub> H <sub>11</sub> )
117	100	(C <sub>8</sub> H <sub>5</sub> O)
133	38	(C <sub>8</sub> H <sub>5</sub> O <sub>2</sub> )
147	55	(C <sub>9</sub> H <sub>7</sub> O <sub>2</sub> )
194	30	(C <sub>14</sub> H <sub>12</sub> N)
206	38	(C <sub>15</sub> H <sub>12</sub> N)
236	13	(C <sub>16</sub> H <sub>14</sub> NO)
284	5	(C <sub>20</sub> H <sub>14</sub> NO)
326	12	(C <sub>22</sub> H <sub>16</sub> NO <sub>2</sub> )
398	8	(C <sub>24</sub> H <sub>22</sub> N <sub>4</sub> O <sub>2</sub> )
438	5	(C <sub>26</sub> H <sub>22</sub> N <sub>4</sub> O <sub>3</sub> )



## ii. Mass spectrum of Cu(II) complex (5)

m/z	Rel. Int.	Fragment
30	39	(C <sub>2</sub> H <sub>6</sub> )
41	24	(C <sub>3</sub> H <sub>5</sub> )
57	27	(C <sub>4</sub> H <sub>9</sub> )
63	11	(C <sub>3</sub> H <sub>11</sub> O)
81	11	(C <sub>4</sub> H <sub>17</sub> O)
98	12	(C <sub>5</sub> H <sub>8</sub> NO)
118	10	(C <sub>6</sub> H <sub>16</sub> NO)
180	6	(C <sub>9</sub> H <sub>12</sub> N <sub>2</sub> O <sub>2</sub> )
198	8	(C <sub>10</sub> H <sub>18</sub> N <sub>2</sub> O <sub>2</sub> )
228	12	(C <sub>11</sub> H <sub>20</sub> N <sub>2</sub> O <sub>3</sub> )
250	25	(C <sub>14</sub> H <sub>22</sub> N <sub>2</sub> O <sub>2</sub> )
279	8	(C <sub>16</sub> H <sub>11</sub> N <sub>2</sub> O <sub>3</sub> )
322	100	(C <sub>19</sub> H <sub>18</sub> N <sub>2</sub> O <sub>3</sub> )
337	11	(C <sub>20</sub> H <sub>21</sub> N <sub>2</sub> O <sub>3</sub> )
365	13	(C <sub>20</sub> H <sub>19</sub> N <sub>3</sub> O <sub>4</sub> )
393	26	(C <sub>21</sub> H <sub>19</sub> N <sub>3</sub> O <sub>5</sub> )
412	10	(C <sub>21</sub> H <sub>19</sub> CuNO <sub>4</sub> )
438	9	(C <sub>22</sub> H <sub>19</sub> CuN <sub>2</sub> O <sub>4</sub> )
517	5	(C <sub>24</sub> H <sub>28</sub> CuN <sub>3</sub> O <sub>6</sub> )
571	12	(C <sub>26</sub> H <sub>28</sub> CuN <sub>4</sub> O <sub>7</sub> )

## ii. Mass spectrum of Zn(II) complex (15)

m/z	Rel. Int.	Fragment
18	37	(CH <sub>6</sub> )
28	90	(C <sub>2</sub> H <sub>4</sub> )
44	13	(C <sub>3</sub> H <sub>8</sub> )
65	8	(C <sub>5</sub> H <sub>5</sub> )
77	9	(C <sub>6</sub> H <sub>5</sub> )
93	7	(C <sub>7</sub> H <sub>9</sub> )
109	15	(C <sub>8</sub> H <sub>13</sub> )
141	11	(C <sub>9</sub> H <sub>17</sub> O)
169	10	(C <sub>10</sub> H <sub>17</sub> O <sub>2</sub> )
195	62	(C <sub>12</sub> H <sub>19</sub> O <sub>2</sub> )



212	92	(C <sub>12</sub> H <sub>20</sub> O <sub>3</sub> )
226	6	(C <sub>12</sub> H <sub>20</sub> NO <sub>3</sub> )
251	36	(C <sub>14</sub> H <sub>21</sub> NO <sub>3</sub> )
265	12	(C <sub>14</sub> H <sub>21</sub> N <sub>2</sub> O <sub>3</sub> )
304	14	(C <sub>17</sub> H <sub>24</sub> N <sub>2</sub> O <sub>3</sub> )
321	15	(C <sub>17</sub> H <sub>25</sub> N <sub>2</sub> O <sub>4</sub> )
337	13	(C <sub>17</sub> H <sub>25</sub> N <sub>2</sub> O <sub>5</sub> )
359	25	(C <sub>25</sub> H <sub>15</sub> N <sub>2</sub> O)
395	100	(C <sub>28</sub> H <sub>15</sub> N <sub>2</sub> O)
413	14	(C <sub>28</sub> H <sub>17</sub> N <sub>2</sub> O <sub>2</sub> )
448	15	(C <sub>28</sub> H <sub>20</sub> N <sub>2</sub> O <sub>4</sub> )
547	12	(C <sub>28</sub> H <sub>24</sub> N <sub>3</sub> O <sub>5</sub> Zn)
577	13	(C <sub>29</sub> H <sub>26</sub> N <sub>3</sub> O <sub>6</sub> Zn)
607	40	(C <sub>30</sub> H <sub>28</sub> N <sub>3</sub> O <sub>7</sub> Zn)
639	20	(C <sub>30</sub> H <sub>30</sub> N <sub>4</sub> O <sub>8</sub> Zn)
657	14	(C <sub>30</sub> H <sub>32</sub> N <sub>4</sub> O <sub>9</sub> Zn)

### 3.3. <sup>1</sup>H-NMR spectra

The <sup>1</sup>H-NMR spectra of the ligand [H<sub>2</sub>L] (1), Cd(II) complex (14) and Zn(II) complex (15) in deuterated DMSO recorded signals consistent with the proposed structures (Figure 2). The ligand showed a three singlet peaks at 11.2 [2H], 9.0 [H] and 8.35 [2H] ppm corresponding to the two protons of the OH, one proton of NH and two protons of N=CH groups respectively [37-39]. The multiplet peaks observed in the 6.94- 7.71 ppm range are assigned to the aromatic protons [11], whereas the singlet signal observed at 2.5 ppm, is due to the two protons of the CH<sub>2</sub> group [40,41]. However, The spectrum of Cd(II) complex (14) showed two singlet peaks at 11.2 and 11.0 ppm assigned to non-coordinated and coordinated protons of OH groups respectively. The singlet peak observed at 8.5 ppm was assigned to the two protons of NH groups, whereas the multiplet peaks appeared in the 6.94- 7.71 ppm range could be assigned to the aromatic protons. The two singlet signals observed at 8.31 and 2.51 ppm were assigned to N=CH and CH<sub>2</sub> groups respectively with intensities corresponding to four protons, whereas the two singlet signals corresponding to the six protons of the acetate groups were observed as singlet peaks at 1.9 ppm and 2.1 ppm [42-44]. Spectrum of Zn(II) complex (15) showed a singlet signal at 11.1 ppm due to two protons of the OH groups; another signal was observed at 9.0 ppm corresponding to one proton of the NH group. However the aromatic signals was observed in the 6.5-7.71 ppm range. The azomethine (CH=N) protons were observed as a singlet peaks at 8.49 and 8.40 ppm whereas the signal observed at 2.49 ppm was assigned to protons of CH<sub>2</sub> group. The signals observed as two singlet peaks at 1.98 and 2.02 ppm ascribed to the six protons of acetate groups [42-44].

### 3.4. Infrared Spectra

Important spectral bands of the ligand and its complexes are presented in table 2. The IR spectrum of the ligand showed broad, medium intensity bands in the 3650–3310 and 3280-2650 cm<sup>-1</sup> ranges, which are attributed to intra- and intermolecular hydrogen bondings [45,46]. The broad medium bands at 3465 and 3436 cm<sup>-1</sup> are assigned to the (OH) group, whereas the relatively strong bands located at 3220, 1623, 1618 and 1316 cm<sup>-1</sup>, are assigned to the ν(NH), phenolic ν(C=N), ν(C=N) and ν(COH) vibrations respectively [47]. Also, the spectrum showed a band at 1031 cm<sup>-1</sup> which is assigned to ν (N-N) vibration [48,49]. In order to study the binding mode of the Schiff base to the metal ion in the complexes, the IR spectrum of the free Schiff base was compared with the spectra of the metal complexes. The spectral data together with the elemental analyses indicated that, the ligand can behave as: Bibasic tetradentate ligand: coordinating through the two O and the two C=N groups as in complexes (2), (4), and (5). This mode of coordination is supported by the evidences: (i) the disappearance of the band for the phenolic OH, indicating the subsequent deprotonation of the phenolic proton prior to coordination [50]. (ii) The strong bands observed for the free Schiff base around 1623 and 1618 cm<sup>-1</sup>, characteristic of the azomethine (C=N) stretching vibrations were shifted to lower wave numbers, suggesting coordination of the azomethine nitrogen atoms to the metal ion [51,52] (iii) The red shift of the phenolic CO vibration band toward lower wave number indicating that, the coordination also takes place through the deprotonated phenolic groups [53,54]. (iii) The appearance of new bands in the 453-565 and 587-590 cm<sup>-1</sup> regions which are assigned to u(M-N) and u(M-O) vibrations respectively [55]. Monobasic tetradentate ligand: In complexes (3), (7), (8), (11), (12)



and **(16)**, each of the two moieties of the ligand participating in the metal complexes coordinating through one O<sup>-</sup>, two C=N and one OH group, this mode of coordination was supported by the evidences: (i) One vibration band of the two C=N was shifted to lower wave number with a decreasing in its intensity while the other one band appeared in its original place [51,52]. (ii) One of the two OH vibrations bands disappeared in the time that the other one shifted to lower wave number with decreasing its intensity [50]. This indicates that, only one atom of each phenolic oxygens and azomethine nitrogens was involved in the metal coordination. (iii) One band of the two C-O bands was shifted to a higher wave number, while the other was found almost at its original place, indicating that, only one phenolic oxygen was involved in the coordination [53,54,56]. (iv) The appearance of new bands in the 564-565 and 575-618 cm<sup>-1</sup> regions are due to the u(M-N) and u(M-O) vibrations respectively [55]. Neutral bidentate ligand: coordinating through one OH and one C=N group as in complexes **(6)**, **(9)** and **(14)**. This mode of coordination is supported by the following evidences: (i) One band of each of OH and C=N group was shifted to a lower wave number with a decreasing its intensity, while the other ones are found almost at their original place, indicating that, only one of each pair were involved in the coordination [50]. (ii) One band of the two C-O bands was shifted to a higher wave number while the other is found almost at its original place, indicating that, only one phenolic oxygen was involved in the coordination [56]. (iii) The appearance of new bands in the 450-550 and 546-565 cm<sup>-1</sup> regions are due to the u(M-N) and u(M-O) vibrations respectively [55]. Monobasic bidentate ligand: coordinating through one O<sup>-</sup> and one C=N groups as in complexes **(10)**, **(13)**, **(17)**, **(18)**, and **(19)**. This mode of coordination is supported by (i) One of two OH vibrations bands disappeared in the time that the other one appeared at its original place [50]. (ii) One vibration band of the two C=N was shifted to lower wave number with a decreasing its intensity while the other one band appeared in its original place. (iii) One band of the two C-O bands was shifted to a higher wave number while the other is found almost at its original place, indicating that, only one phenolic oxygen was involved in the coordination [53,54]. (iv) The appearance of new bands in the 459-550 and 546-600 cm<sup>-1</sup> regions are due to the u(M-N) and u(M-O) vibrations respectively [55]. Neutral tetradentate ligand: coordinating through two OH and two C=N groups as in complex **(15)**. This mode of coordination is supported by (i) The two vibration bands of each of OH and C=N were shifted to lower wave number with a decreasing in their intensities [50]. (ii) The two bands C-O vibrations were shifted to a higher wave number, indicating participation of the two phenolic oxygen in the metal coordination. (iv) The appearance of new bands in the 420-550 and 455-605 cm<sup>-1</sup> regions corresponding to the u(M-N) and u(M-O) vibrations respectively [55]. The presence of water molecules within the coordination sphere in all complexes except **(6)**, **(9)**, **(14)** and **(15)** were supported by the presence of weak bands around 3560-3380 cm<sup>-1</sup>, 1600-1595 cm<sup>-1</sup>, 895-943 cm<sup>-1</sup> and 645-665 cm<sup>-1</sup> due to OH stretching, HOH deformation, H<sub>2</sub>O rocking and H<sub>2</sub>O wagging, respectively [57,58]. The appearance of two characteristic bands in the 1471-1435 and 1341-1330 cm<sup>-1</sup> ranges in the spectra of complexes **(9)**, **(14)**, **(15)** and **(19)** were attributed to  $\nu_{\text{asym}}(\text{COO}^-)$  and  $\nu_{\text{sym}}(\text{COO}^-)$  respectively, indicating the participation of the acetate oxygen in the complex formation [59]. The coordination modes of the acetate group in the complexes were determined by IR spectra, by comparing the separations between the  $\nu_{\text{asym}}(\text{COO}^-)$  and  $\nu_{\text{sym}}(\text{COO}^-)$ . The separation value ( $\Delta$ ) between  $\nu_{\text{asym}}(\text{COO}^-)$  and  $\nu_{\text{sym}}(\text{COO}^-)$  for these complexes were in the range 105-130 cm<sup>-1</sup>, suggesting a monodentate coordination fashion of the acetate groups [60,61]. The spectra of complexes **(6)** and **(12)** showed bands in the 1330-1327, 1148-1128, 894-890 and 785-752 cm<sup>-1</sup> ranges corresponding to coordinating nitrate group in a unidentate mode [62-64]. Complexes **(11)** and **(16)** spectra demonstrated strong to medium bands at 1206, 1195, 1156, 1147, 1140, 682, 681 and 458 cm<sup>-1</sup> belonging to the antisymmetric and symmetric stretching modes of the sulfate group. These values are consistent with that reported for the sulfate species coordinating to the M(II) in an unidentate fashion [64,38]. Complexes **(7)** showed additional band at 415 cm<sup>-1</sup> assigned to a coordinated chloride atom.

### 3.5. Electronic spectra and magnetic moments.

DMF electronic absorption spectral bands as well as, room temperature effective magnetic moment values of the ligand and its metal complexes are reported in table 3. The ligand showed three transition bands in the high energy region. The first band appeared at 290 nm is assigned to  $\pi \rightarrow \pi^*$  transition within the aromatic rings and this band is nearly unchanged upon complexation. The second and third bands appearing at 315 and 350 nm may be assigned to  $n \rightarrow \pi^*$  of the azomethine groups and CT transitions [65,66]. The bands were found to be shifted upon complexation indicating involvement of these transition in the coordination with the metal ions. The electronic spectra of the Co(II) complex **(2)** and **(13)** exhibit three d-d transition bands at 720, 715; 610, 620, and 560, 550. These bands are assigned to  ${}^4T_{1g}(F) \rightarrow {}^4T_{2g}(F)_{(1)}$ ,  ${}^4T_{1g}(F) \rightarrow {}^4T_{1g}(P)_{(2)}$ ,  ${}^4T_{1g}(F) \rightarrow {}^4A_1(F)_{(3)}$  transitions respectively, corresponding to high spin cobalt(II) octahedral complexes [66,67]. The magnetic moment of complex **(2)** is 4.98, and 4.74 B.M. B.M., which is well within the reported range of high spin octahedral Co(II) complexes. Electronic spectra of Co(II) complex **(11)** show bands at 570 and 610 nm. These bands are assigned to  ${}^4A_{2g}(F) \rightarrow {}^4T_{2g}(P)_{(3)}$  and  ${}^4A_{2g}(F) \rightarrow {}^4T_1(F)_{(2)}$  transitions respectively corresponding to cobalt(II) tetrahedral complexes. The value of the room temperature magnetic moments of complexes **(11)** is 3.88 B.M., the decrease in the observed magnetic moment (3.88 B.M.) is assigned to spin-spin interactions taking place between Co(II) ions. The electronic absorption spectra of Ni(II) complexes **(3)** and **(4)** displayed three bands at 725-740 and 608-615 nm, these bands are corresponding to  ${}^3A_{2g}(F) \rightarrow {}^3T_{2g}(F)_{(1)}$ ,  ${}^3A_{2g}(F) \rightarrow {}^3T_{1g}(F)_{(2)}$  and  ${}^3A_{2g}(F) \rightarrow {}^3T_{1g}(P)_{(3)}$  transitions respectively, indicating octahedral nickel(II) complexes [68,69]. The lower value of  $d/d_1$  ratio for the complexes (1.20-1.21) range which are less than the usual range of 1.5-1.75, indicating distorted octahedral nickel(II) complexes [68,69]. The magnetic moment values of for nickel(II) complexes **(3)** and **(4)** are 2.15 and 3.05 BM respectively, which are consistent with two unpaired electrons state and confirming octahedral geometry for around the nickel(II) ion [68]. The electronic spectra of copper(II) complexes **(5)**, **(7)**, **(12)** and **(16)** exhibited bands in the 605-620 and 575-590 nm ranges which are assigned to  ${}^2B_{1g}A_{1g}(d_{x^2-y^2} \rightarrow d_{z^2})$ , and  ${}^2B_{1g}E_g(d_{x^2-y^2} \rightarrow d_{xy}, d_{yz})$  transitions respectively. These transitions indicate that, the copper(II) ion has a tetragonally distorted octahedral geometry. This could be due to the Jahn-Teller effect that operates on the  $d^9$  electronic ground state of six coordinate system, elongating one trans pair of coordinate bonds and shortening the remaining four ones [40, 43]. The electronic spectrum of complex **(7)** showed peaks at 575 and 620 nm. These bands are assigned to  ${}^2B_{1g}^2B_{2g}$  and  ${}^2B_{1g}^2A_{1g}$  transitions, indicating a square planar copper(II) complexes [55,70]. The magnetic moments for all copper(II) complexes at room temperature are in the 1.66-1.74 B.M. range, indicating that, the complexes have octahedral or square planar geometry [71]. The apparent lower values of complexes **(12)** and **(16)** may be assigned to spin-spin interactions



take place between copper(II) ions through molecular interactions[71]. The absorption spectrum of manganese(II) complex (10) showed bands at 585 and 610 nm. These two bands can be assigned to  ${}^5B_{1g} \rightarrow {}^5E_g$  and  ${}^6B_{1g} \rightarrow {}^6A_{2g}$  transitions respectively, suggesting an distorted octahedral arrangement around the manganese(II) ion [72,73]. The magnetic moment value for the complex (10) is 5.08 B.M., which is consistent with a high spin octahedral geometry around the manganese(II) ion [74,72]. Diamagnetic cadmium(II), zinc(II), mercury(II), strontium(II), thallium(II) and silver(I) complexes showed only intraligand transitions and (LMCT) (Table 4).

**Table 4:- Electronic Spectra (nm) and Magnetic Moments (B.M) for the Ligand,(1) and its metal Complexes.**

Comp. No.	( $\lambda_{\max}$ (nm	(BM) <sub>eff</sub>	1/2
(1)	290,315,350	-	-
(2)	290,310,330,450,560,610,720	4.98	1.18
(3)	285,307,328,465,575,608,735	2.15	1.21
(4)	285,305,325,495,550,615,740	3.05	1.2
(5)	285,310,336,465,585,615	1.74	-
(6)	285,295,325,365	Diamagnetic	-
(7)	290,315,327,435,575,620	1.63	-
(8)	285,305,325,406,590,625	Diamagnetic	-
(9)	300,326 ,285	Diamagnetic	-
(10)	285,310,325,490,585,610	5.08	-
(11)	480,570,610 ,285,300,335	3.88	-
(12)	290,310,330,465,590,605	1.65	-
(13)	550,620,715 ,290,310,335,490	4.74	-
(14)	335 ,285,305	Diamagnetic	-
(15)	285,305,330	Diamagnetic	-
(16)	465,590,610 ,285,310,325	1.66	-
(17)	340 ,285,305	Diamagnetic	-
(18)	305,335 ,285	Diamagnetic	-
(19)	305,335,410 ,285	2.03	-

### 3.6. Electron spin resonance (ESR)

The ESR spectral data for metal complexes (2), (3), (5), (7), (8), (10), (11), (12), (13) and (16) are presented in table 5. Complex (3) showed broad signal in the low and high field regions indicating spin-exchange interactions take place between Ni(II) ions which is confirmed by the magnetic moment value. The spectra of copper(II) metal complexes (5), (7), (12) and (16) are characteristic of species,  $d^9$  configuration and having axial type of a  $d(x^2-y^2)$  ground state which is the most common for copper(II) complexes [75,76]. The metal complexes showed  $g_{\parallel} \gg 2.0023$ , indicating octahedral geometry around the copper(II) ion [77]. The expression  $G$  is related to  $g$ -values,  $G = (g_{\parallel}-2)/(g_{\perp}-2)$ . If  $G > 4.0$ , then local tetragonal axes are misaligned parallel or only slightly misaligned and if  $G < 4.0$ , significant exchange coupling is present [78]. Metal complexes (12) and (16) showed values indicating spin-exchange interactions take place between the copper(II) ions, which is consistent with the of magnetic moments values (Table 4). Also, the  $g_{\parallel}/A_{\parallel}$  values are considered as a diagnostic of stereochemistry. The  $g_{\parallel}/A_{\parallel}$  values lie just within the range expected for the octahedral metal complexes [79]. The orbital reduction factors ( $K_{\parallel}$ ,  $K_{\perp}$ ,  $K_{\sigma}$ ), which are a measure of covalency were also calculated [80].  $K$  values, for the copper(II) complexes (5), (7), (12) and (16), indicating covalent bond character [80]. Also, the  $g$ -values show considerable a covalent bond character. The in-plane  $\sigma$ -covalency parameter,  $\alpha^2$  (Cu) suggests a covalent bonding. The complexes show  $\beta_1^2$  values indicating a covalency character in the in-plane  $\pi$ -bonding. While  $\beta^2$  for the complexes indicating a covalent bonding character in the out of plane  $\pi$ -bonding except complexes (12) and (16) which indicate ionic bond character [81,78]. The calculated orbital populations ( $a^2d$ ) for the copper(II) complexes indicate a  $d(x^2-y^2)$  ground state [82]. Cobalt(II) complexes (2), (11) and (13), Iron(II) complex (8) and manganese(II) complex (10), show isotropic spectra.



### 3.7. Thermal analyses (DTA and TGA)

The thermal data of metal complexes (**3**), (**4**), (**8**), (**12**), (**13**), (**15**) and (**16**) were presented in table 6. The thermal curves in the 27-800°C temperature range indicated that the metal complexes are thermally stable up to 40 °C. The weight losses recorded in the 70-90°C range is due to elimination of hydrated water molecules. Ni(II) complex (**3**) showed an endothermic peak at 50°C due to broken of the hydrogen bondings. Another endothermic peak was observed at 80°C, with 2.38% weight loss (Calc. 2.53%) corresponding to loss of two hydrated water molecules. The loss of coordinated water molecules was accompanied by three endothermic peaks at 120, 135, and 155 °C with weight losses 2.72%(Calc. 2.59%), 4.1% (Calc. 3.99%) and 4.33% (Calc. 4.16%) which were assigned to removal of two, three and three coordinated water molecules respectively. The endothermic peak observed at 230°C, with 8.16%weight loss (Calc. 8.36%) is due to loss of one terminal coordinated SO<sub>4</sub> group, whereas, the loss of the other terminal coordinated SO<sub>4</sub> group was accompanied by an endothermic peak at 250°Cwith 8.84%weight loss (Calc. 9.13%). The endothermic peak observed at 315°C, is corresponding to the melting point of the complex. Finally, the complex shows multiple exothermic peaks at 370, 390, 420, 450 and 500°C, with total 23.13%weight loss (Calc. 23.56%) corresponding to the thermal decomposition of the complexes with the eventually formation of three NiO molecules. Ni(II) complex (**4**) thermogram showed an endothermic peak at 45°C due to broken of the hydrogen bondings. An endothermic peak was observed at 80°C, with 6.33%weight loss (Calc. 6.35%) corresponding to loss of two hydrated water molecules. The endothermic peak observed at 150°C, with 6.69%weight loss (Calc. 6.78%) is due to loss of two coordinated water molecules. The endothermic peak observed at 360°C, is corresponding to melting point of the complex. Finally, the complex showed multiple exothermic peaks at 405, 450, 485, 510 and 530°C, with total 14.72%weight loss (Calc. 15.0%) corresponding to thermal decomposition with eventually formation of one NiO molecule. The thermogram of Fe(II) complex (**8**) showed an endothermic peak at 50°C, due to broken of the hydrogen bondings. An endothermic peak was observed at 85°C, with 1.41% weight losses (Calc. 1.29%) corresponding to loss of hydrated water molecule. The loss of coordinated water molecules was accompanied by three endothermic peaks at 115, 125, and 155 °C with weight losses 2.81% (Calc. 2.61%),4.78% (Calc. 4.02%) and 4.57% (Calc. 4.19%) which were assigned to removal of two middle, three terminal and three terminal coordinated water molecules respectively. The endothermic peak observed at 250°C with 7.74%weight loss (Calc. 7.77%), was assigned to loss of one terminal coordinated SO<sub>4</sub> group. The loss of other terminal coordinated SO<sub>4</sub> group was accompanied with an endothermic peak at 300°C with 8.45%weight loss (Calc. 8.43%). An endothermic peak was observed at 325°C which could be assigned to the melting point. Finally, the complex shows multiple exothermic peaks at 350, 380, 450, 500 and 610°C, with total 21.83% weight loss (Calc. 21.95%) corresponding to thermal decomposition with the formation of Fe<sub>3</sub>O<sub>4</sub> molecule. The thermogram of Cu(II) complex (**12**) showed an endothermic peak at 45°Cdue to broken of hydrogen bondings. The endothermic peak observed at 78°C, with 5.63%weight loss (Calc. 5.83%) was assigned to loss of two hydrated water molecules. Whereas the endothermic peak observed at 165°C, with 3.52% weight loss (Calc. 3.10%) was ascribed to loss of a coordinated water molecule. Another endothermic peak was observed at 235°C, with 11.27%weight loss (Calc. 11.01%), which is assigned to loss of coordinated NO<sub>3</sub> group. The endothermic peak observed at 330°C, is corresponding to the melting point of the complex. The complex showed multiple exothermic peaks at 370, 410, 435 and 500°C, with total 13.73%weight loss (Calc. 14.03%) corresponding to thermal decomposition with the final formation of one CuO molecule. The thermogram of Co(II) complex (**13**) showed endothermic peak at 45°C, due to broken of hydrogen bondings. Two endothermic peaks observed at 80°C and 90°C with 3.52%weight loss (Calc. 3.38%), corresponding to loss of two hydrated water molecules. The loss of two coordinated water molecules was accompanied by an endothermic peak observed at 130°C, with 3.24% weight loss (Calc. 3.49%). The melting point of the complex appears at 325°C as an endothermic peak. Multiple exothermic peaks were observed at 365, 450, 550 and 600°C with total 7.74% weight loss (Calc. 7.54%) due to thermal decomposition of the complex with the final formation of one CoO molecule. The thermogram of Zn(II) complex (**15**) showed an endothermic peak at 45°C, corresponding to broken of hydrogen bondings, whereas, the endothermic peak observed at 70°C, with 2.46% weight loss (Calc. 2.73%) was assigned to loss of two hydrated water molecules. The loss of two acetate groups was accompanied by two endothermic peaks at 210 and 225 °C with 18.33%weight loss (Calc. 18.97%). An endothermic peak was observed at 345°C, corresponding to the melting point of the complex. Finally, multiple exothermic peaks was observed at 370, 390, 410, 450 and 510°C, with total 16.67%weight loss (Calc. 16.1%), assigned to thermal decomposition process with the formation of one ZnO molecule. The thermogram of Cu(II) complex (**16**) showed an endothermic peak at 50°Cdue to broken of hydrogen bondings, whereas the loss of one hydrated water molecule was accompanied with endothermic peak at 90°C with 1.41% weight loss (Calc. 1.27%).The loss of coordinated water molecules was accompanied by three endothermic peaks at 130, 150, and 170 °C with weight losses 2.13% (Calc. 2.57%), 4.25% (Calc. 3.95%) and 3.83% (Calc. 4.11%) which were assigned to removal of two middle, three terminal and three terminal coordinated water molecules respectively. An endothermic peak was observed at 215°C with 7.80% weight loss (Calc. 7.63%) which could be assigned to loss of a coordinated SO<sub>4</sub> group, whereas, the loss the other sulfate group was accompanied with an endothermic peak at 230°C with 8.51% weight loss (Calc. 8.26%). The endothermic peak observed at 360°C was assigned to the melting point of the complex. Thermal decomposition of the complex was accompanied by multiple exothermic peaks at 390, 430, 510, 530 and 630°C with total 21.98% weight loss (Calc. 22.23%) with final formation of three CuO molecules.



Table 5:- ESR data for metal (II) complexes

Complex	g	g	$g_{iso}^a$	A (G)	A (G)	$A_{iso}^b$ (G)	$G^c$	$\Delta E_{xy}$ (cm <sup>-1</sup> )	$\Delta E_{xz}$ (cm <sup>-1</sup> )	$K^2$	$K^2$	$K^2$	K	g/A (cm <sup>-1</sup> )	$\alpha^2$	$\beta^2$	$\beta_1^2$	-2 $\beta$	a <sup>2</sup> d(%)
(2)	-	-	2.13	-	-	-	-	-	-	-	-	-	-	-	-	-	-	-	-
(5)	2.26	2.04	2.11	130	10	50	6.5	17094	21505	0.49	0.66	0.54	0.73	165	0.68	0.72	0.97	190.5	81
(7)	2.22	2.07	2.12	180	15	70	3.14	17391	22988	0.71	0.75	0.74	0.86	123.3	0.88	0.80	0.85	126.6	54
(8)	-	-	2.09	-	-	-	-	-	-	-	-	-	-	-	-	-	-	-	-
(10)	-	-	2.01	-	-	-	-	-	-	-	-	-	-	-	-	-	-	-	-
(11)	-	-	2.11	-	-	-	-	-	-	-	-	-	-	-	-	-	-	-	-
(12)	2.71	2.06	2.09	150	15	60	2.83	16949	21505	0.75	0.43	0.64	0.8	144.7	0.65	1.15	0.66	162.8	69.3
(13)	-	-	2.09	-	-	-	-	-	-	-	-	-	-	-	-	-	-	-	-
(16)	2.18	2.05	2.09	125	12.5	50	3.6	16949	21505	0.62	0.45	0.56	0.75	171.6	0.59	1.05	0.76	127.1	54

a)  $3g_{iso} = g + 2g_{\perp}$

b)  $3A_{iso} = A + 2A_{\perp}$

c)  $G = g - 2/g_{\perp} - 2$



**Table 6:- Thermal analyses for metal (II) complexes**

No.	Temp. (oC)	DTA (peak)		TGA (Wt.loss %)		Assignments
		Endo	Exo	Calc.	Found	
(3)	50	Endo	-	-	-	Broken of H-bondings
	80	Endo	-	2.53	2.38	Loss of (2H <sub>2</sub> O) hydrated water molecules
	120	Endo	-	2.59	2.72	Loss of (2H <sub>2</sub> O) middle coordinated water molecules
	135	Endo	-	3.99	4.1	Loss of (3H <sub>2</sub> O) Terminal coordinated water molecules
	155	Endo	-	4.16	4.33	Loss of (3H <sub>2</sub> O) Terminal coordinated water molecules
	230	Endo	-	8.36	8.16	Loss of coordinated SO <sub>4</sub> group
	250	Endo	-	9.13	8.84	Loss of coordinated SO <sub>4</sub> group
(3)	315	Endo	-	-	-	Melting point
	370,390,420,450,500	-	Exo	23.56	23.13	Decomposition process with the formation of 3NiO
(4)	45	Endo	-	-	-	Broken of H-bondings
	80	Endo	-	6.35	6.33	Loss of (2H <sub>2</sub> O) hydrated water molecules
	150	Endo	-	6.78	6.69	Loss of (2H <sub>2</sub> O) coordinated water molecules
(8)	360	Endo	-	-	-	Melting point
	405,450,485,510,530	-	Exo	15.0	14.72	Decomposition process with the formation of NiO
	50	Endo	-	-	-	Broken of H-bondings
	85	Endo	-	1.29	1.41	Loss of (H <sub>2</sub> O) hydrated water molecule
	115	Endo	-	2.61	2.81	Loss of(2H <sub>2</sub> O) middle coordinated water molecules
	125	Endo	-	4.02	4.78	Loss of (3H <sub>2</sub> O) terminal coordinated water molecules
	150	Endo	-	4.19	4.57	Loss of (3H <sub>2</sub> O) terminal coordinated water molecules
	250	Endo	-	7.77	7.74	Loss of coordinated terminal SO <sub>4</sub> group
	300	Endo	-	8.43	8.45	Loss of coordinated terminal SO <sub>4</sub> group
	325	Endo	-	-	-	Melting point
	350,380,450,500,610	-	Exo	21.95	21.83	Decomposition process with the formation of Fe <sub>3</sub> O <sub>4</sub>
(12)	45	Endo	-	-	-	Broken of H-bondings
	78	Endo	-	5.83	5.63	Loss of (2H <sub>2</sub> O) hydrated water molecules
	165	Endo	-	3.10	3.52	Loss of coordinated H <sub>2</sub> O molecule
	235	Endo	-	11.01	11.27	Loss of coordinated NO <sub>3</sub> group
	330	Endo	-	-	-	Melting point
(12)	370,410,435,500	-	Exo	14.03	13.73	Decomposition process with the formation of CuO
(13)	45	Endo	-	-	-	Broken of H-bondings
	80,90	Endo	-	3.38	3.52	Loss of (2H <sub>2</sub> O) hydrated water molecules
	130	Endo	-	3.49	3.24	Loss of (2H <sub>2</sub> O) coordinated water molecules
	325	Endo	-	-	-	Melting point
(13)	365,450,550,600	-	Exo	7.54	7.74	Decomposition process with the formation of CoO
(15)	45	Endo	-	-	-	Broken of H-bondings
	70	Endo	-	5.51	5.35	Loss of 2(H <sub>2</sub> O) hydrated water molecules
	210,225	Endo	-	18.97	18.33	Loss of coordinated 2(OAc) group
(15)	345	Endo	-	-	-	Melting Point





<b>(16)</b>	370,390,410,450,510	-	Exo	16.1	16.67	Decomposition process with the formation of ZnO
	45	Endo	-	-	-	Broken of H-bondings
	50	Endo	-	-	-	Broken of H-bondings
	90	Endo	-	1.27	1.41	Loss of hydrated H <sub>2</sub> O
	130	Endo	-	2.57	2.13	Loss of (2H <sub>2</sub> O) middle coordinated water molecules
	150	Endo	-	3.95	4.25	Loss of (3H <sub>2</sub> O) terminal coordinated water molecules
	170	Endo	-	4.11	3.83	Loss of (3H <sub>2</sub> O) terminal coordinated water molecules
	215	Endo	-	7.63	7.80	Loss of coordinated SO <sub>4</sub> group
	230	Endo	-	8.26	8.51	Loss of coordinated SO <sub>4</sub> group
	360	Endo	-	-	-	Melting Point
390,430,510,530,630	-	-	22.23	21.98	Decomposition process with the formation of 3CuO	

### 3.8. Biological studies

#### 3.8.1. Cytotoxic activity

The ligand and some metal complexes were evaluated for their cytotoxicity against two different tumor cell lines (HEP-G2 and HCT-116) by MTT assay using *Vinblastine* as a standard drug. It is interesting to note that, the selected compounds showed cytotoxicity potential in the range of cancerous cell lines tested (Figure 3). The IC<sub>50</sub> values derived from the experimental data were summarized in table 7. It was reported that, compounds exhibiting IC<sub>50</sub> values more than 10–25 µg/ml are treated as weak cytotoxic activities while compounds with IC<sub>50</sub> values less than 5 µg/ml are considered to be very active. Those having intermediate values ranging from 5 to 10 µg/ml are classified as moderately active [83]. The invitro cytotoxicity values demonstrated that, the tested complexes have higher activity in comparison with that of the ligand against (HCT-116) tumor cell lines. Cu(II) complex (5) demonstrated very active cytotoxicity with IC<sub>50</sub> values 2.76 µg/ml, whereas Ni(II) complex (4) showed moderate cytotoxicity with IC<sub>50</sub> values 12.2µg/ml, in the time that the ligand (1) recorded weak cytotoxicity with (IC<sub>50</sub> values 20.1 µg/ml) comparing with the control. The enhancement of cytotoxic activity may be assigned to that the positive charge of the metal increases the acidity of coordinated ligand that bears protons, leading to stronger hydrogen bonds and enhancement of the biological activity [84,85]. It was shown also that, there is a positive correlation between the surviving fraction ratio of tumor cell lines and the metal complexes concentrations. The biological assays of the metal complexes against (HEP-G2) tumor cell lines revealed that, Zn(II) complex (15) exhibits the highest inhibitory ability with IC<sub>50</sub> value equals 5.26 µg/ml. This value is slightly higher when compared with complex (14) (IC<sub>50</sub> 6.13 µg/ml). On the other hand Co(II) complex (2) recorded a weak cytotoxicity with (IC<sub>50</sub> values 24.6 µg/ml) in comparison with the control drug. These findings suggest that both copper(II) complex (5) and Zn(II) complex(15) exhibit promising potentials as an anticancer compounds against (HEP-G2 and HCT-116) tumor cell respectively. (Figure 4, 5)

**Table 7. Cytotoxic activity (IC<sub>50</sub>) of selected metal complexes against human colon carcinoma cells (HCT-116 cell line) and hepatocellular carcinoma cells (HEPG-2 cell line).**

No.	Compound	IC <sub>50</sub> (µg/ml)	
		HEPG-2	HCT-116
(1)	[H <sub>2</sub> L]	-	20.1
(2)	[(L)Co(H <sub>2</sub> O) <sub>2</sub> ].H <sub>2</sub> O	24.6	-
(4)	[(L)Ni (H <sub>2</sub> O) <sub>2</sub> ].2H <sub>2</sub> O	-	12.2
(5)	[(L)Cu(H <sub>2</sub> O) <sub>2</sub> ].2H <sub>2</sub> O	-	2.76
(14)	[(HL) <sub>2</sub> Cd(OAc) <sub>2</sub> ].2H <sub>2</sub> O	6.13	-
(15)	[(H <sub>2</sub> L)Zn(OAc) <sub>2</sub> ].2H <sub>2</sub> O	5.26	-
<b>Standard</b>		4.6	2.38

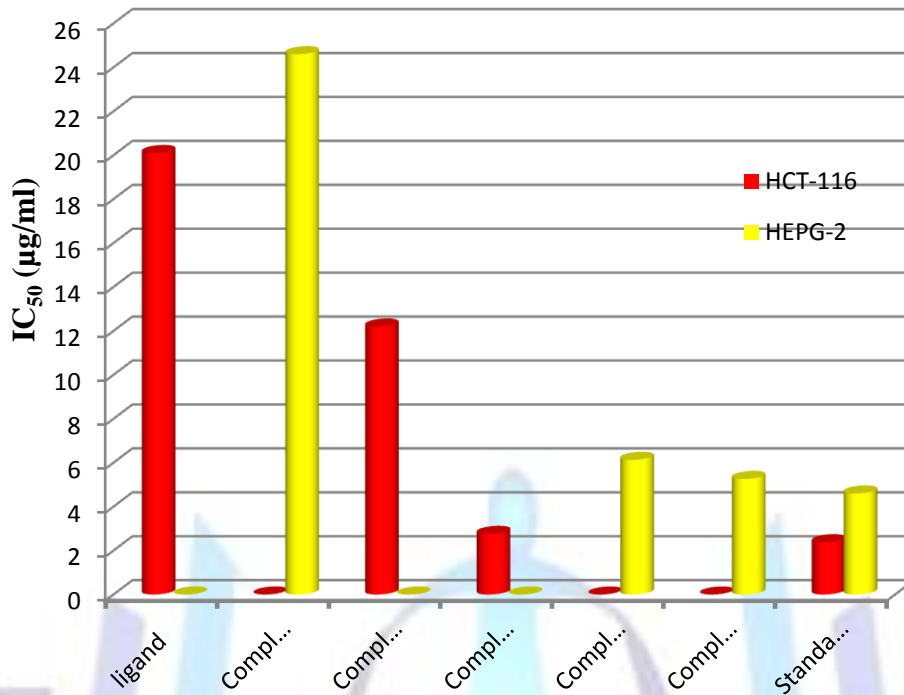


Figure 3: IC<sub>50</sub> values of the ligand [H<sub>2</sub>L] and some metal complexes against human hepatocarcinoma (HEPG-2) and human colon cancer cell lines (HCT-116.)

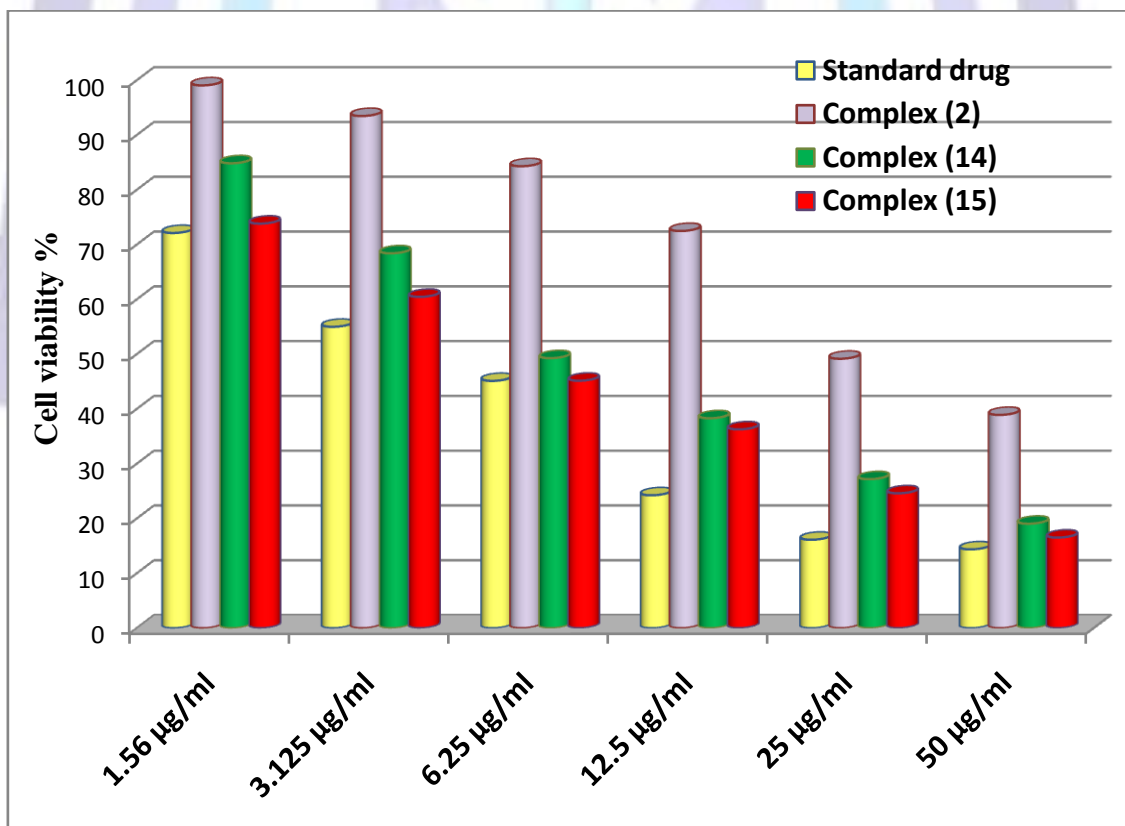


Figure 4: Antiproliferative activity against human hepatocarcinoma (HEPG-2.) at different metal complexes concentrations.

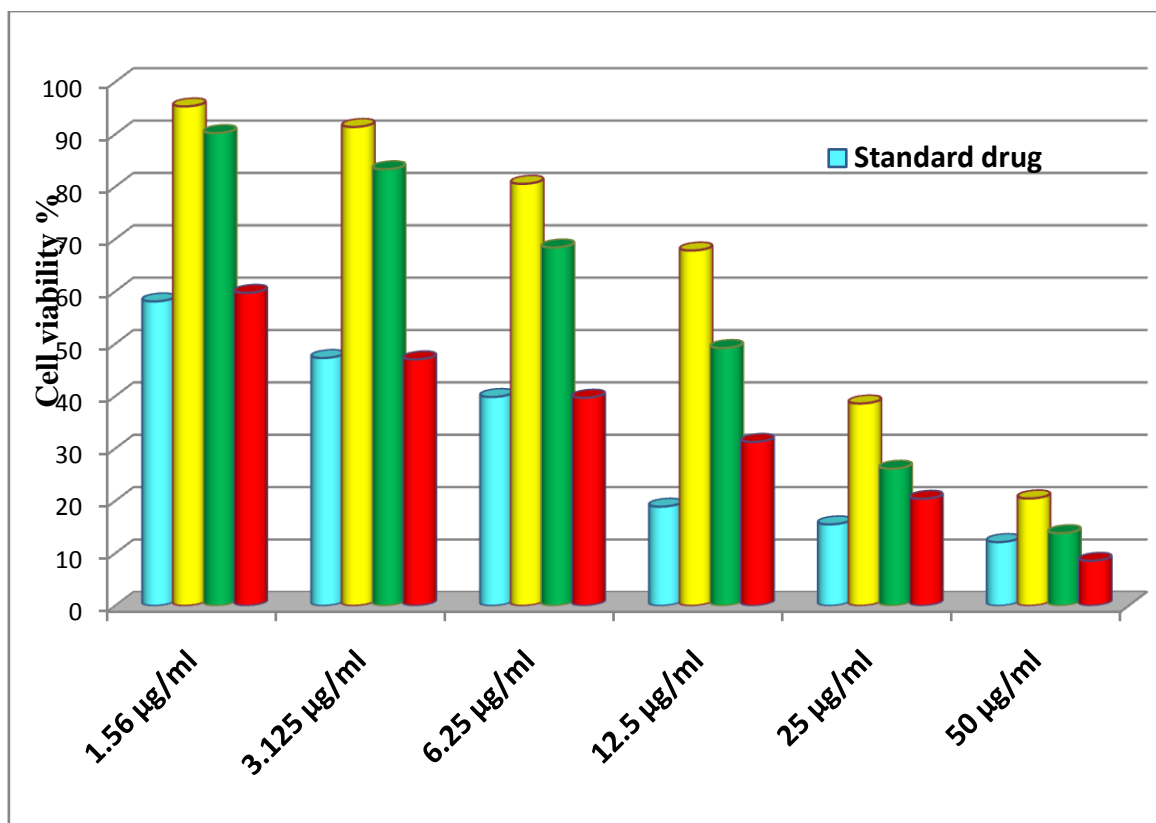


Figure 4. Antiproliferative activity against human colon cell lines (MCT-116) at different the metal complexes concentrations.

#### 4. Conclusion.

The newly synthesized Schiff base ligand derived from (1E, N'Z, N'Z)-N', N'-bis (2-hydroxybenzylidene)-2-(naphthalen-1-yloxy) acetohydrazonehydrazide [H<sub>2</sub>L] act as bidentate or a tetradentatetridentate ligands, and in all complexes was coordinated through the azomethine nitrogen and phenolic oxygen groups to the metal ion. All the synthesized metal(II) complexes possessed an octahedral geometry except the silver complex (6), copper complex (7) and cobalt complexes (11). The reasonable agreement between the theoretical and experimental data reflects to the great extent the suitability of the suggested structures. The invitro cytotoxicity values demonstrated that the tested complexes have higher activity than the ligand against (HCT-116). Copper(II) complex (5) and Zn(II) complex (15) exhibit promising potentials as an anticancer compounds against (HCT-116 and HEP-G2) tumor cell respectively.

#### References

- [1]Radunsky, C., Kösters J., Müller J. 2015. Chromogenic behaviour of a family of hydrazine and hydrazone metal complexes. *InorganicaChimicaActa* 428 (0):14-20.
- [2]Premkumar, T., Govindarajan S. 2002. The chemistry of hydrazine derivatives—thermal behavior and characterisation of hydrazinium salts and metal hydrazine complexes of 4,5-imidazolecarboxylic acid. *ThermochimicaActa* 386 (1):35-42.
- [3]Heaton, B. T., Jacob C., Page P. 1996. Transition metal complexes containing hydrazine and substituted hydrazines. *Coordination Chemistry Reviews* 154 (0):193-229.
- [4]Prakash, G., Manikandan R., Viswanathamurthi P., Velmurugan K., Nandhakumar R. 2014. Ruthenium(III) S-methylisothiosemicarbazone Schiff base complexes bearing PPh<sub>3</sub>/AsPh<sub>3</sub> coligand: Synthesis, structure and biological investigations, including antioxidant, DNA and protein interaction, and in vitro anticancer activities. *Journal of Photochemistry and Photobiology B: Biology* 138 (0):63-74.
- [5]Li, X., Bi C.-f., Fan Y.-h., Zhang X., Meng X.-m., Cui L.-s. 2014. Synthesis, crystal structure and anticancer activity of a novel ternary copper(II) complex with Schiff base derived from 2-amino-4-fluorobenzoic acid and salicylaldehyde. *Inorganic Chemistry Communications* 50 (0):35-41.
- [6]Bhat, M. A., Iqbal M., Al-Dhfyhan A., Shakeel F. 2015. Carvone Schiff base of isoniazid as a novel antitumor agent: Nanoemulsion development and pharmacokinetic evaluation. *Journal of Molecular Liquids* 203 (0):111-119.



- [7]El-Tabl, A. S., Shakhofa M. M. E., Whaba M. A. 2015. Synthesis, characterization and fungicidal activity of binary and ternary metal(II) complexes derived from 4,4'-(4-nitro-1,2-phenylene) bis(azanylylidene))bis(3-(hydroxyimino)pentan-2-one). *SpectrochimicaActa Part A: Molecular and Biomolecular Spectroscopy* 136, Part C (0):1941-1949.
- [8]A. S. Eltabl, M. A.-E., M. A. Wahba, S. A. EL-assaly, L. M. Saad 2014. Sugar Hydrazone Complexes; Synthesis, Spectroscopic Characterization and Antitumor Activity. *Journal of Advances in Chemistry* 9 (1):1837-1860.
- [9]Sun, R. W.-Y., Ma D.-L., Wong E. L.-M., Che C.-M. 2007. Some uses of transition metal complexes as anti-cancer and anti-HIV agents. *Dalton transactions* (43):4884-4892.
- [10]Haas, K. L., Franz K. J. 2009. Application of metal coordination chemistry to explore and manipulate cell biology. *Chemical reviews* 109 (10):4921-4960.
- [11]Correia I1, A. P., Roy S1, Wahba M2, Matos C1, Maurya MR3, Marques F4, Pavan FR5, Leite CQ5, Avecilla F6, Costa Pessoa J7. 2014. Hydroxyquinoline derived vanadium(IV and V) and copper(II) complexes as potential anti-tuberculosis and anti-tumor agents. *J InorgBiochem* 41 (C):83-93.
- [12]Correia, I., Adão P., Roy S., Wahba M., Matos C., Maurya M. R., Marques F., Pavan F. R., Leite C. Q. F., Avecilla F., Costa Pessoa J. 2014. Hydroxyquinoline derived vanadium(IV and V) and copper(II) complexes as potential anti-tuberculosis and anti-tumor agents. *Journal of Inorganic Biochemistry* 141 (0):83-93.
- [13]Fricker, S. P. 2007. Metal based drugs: from serendipity to design. *Dalton transactions* (43):4903-4917.
- [14]Meggers, E. 2009. Targeting proteins with metal complexes. *Chemical Communications* (9):1001-1010.
- [15]Shchepin, R., Navarathna D. H. M. L. P., Dumitru R., Lippold S., Nickerson K. W., Dussault P. H. 2008. Influence of heterocyclic and oxime-containing farnesol analogs on quorum sensing and pathogenicity in *Candida albicans*. *Bioorganic & Medicinal Chemistry* 16 (4):1842-1848.
- [16]Chandra, S., Vandana, Kumar S. 2015. Synthesis, spectroscopic, anticancer, antibacterial and antifungal studies of Ni(II) and Cu(II) complexes with hydrazine carboxamide, 2-[3-methyl-2-thienyl methylene]. *SpectrochimicaActa Part A: Molecular and Biomolecular Spectroscopy* 135 (0):356-363.
- [17]Liang, J.-H., Lv W., Li X.-L., An K., Cushman M., Wang H., Xu Y.-C. 2013. Synthesis and antibacterial activity of 9-oxime ether non-ketolides, and novel binding mode of alkylides with bacterial rRNA. *Bioorganic & Medicinal Chemistry Letters* 23 (5):1387-1393.
- [18]El-Gamal, M. I., Bayomi S. M., El-Ashry S. M., Said S. A., Abdel-Aziz A. A. M., Abdel-Aziz N. I. 2010. Synthesis and anti-inflammatory activity of novel (substituted)benzylidene acetone oxime ether derivatives: Molecular modeling study. *European Journal of Medicinal Chemistry* 45 (4):1403-1414.
- [19]Nirmala, P., Ramanathan M. 2011. Effect of kaempferol on lipid peroxidation and antioxidant status in 1,2-dimethyl hydrazine induced colorectal carcinoma in rats. *European Journal of Pharmacology* 654 (1):75-79.
- [20]Özyürek, M., Akpınar D., Bener M., Türkkan B., Güçlü K., Apak R. 2014. Novel oxime based flavanone, naringin-oxime: Synthesis, characterization and screening for antioxidant activity. *Chemico-Biological Interactions* 212 (0):40-46.
- [21]Wang, R., Zhang X., Song H., Zhou S., Li S. 2014. Synthesis and evaluation of novel alkannin and shikonin oxime derivatives as potent antitumor agents. *Bioorganic & Medicinal Chemistry Letters* 24 (17):4304-4307.
- [22]Dilman, V. M., Anisimov V. N. 1979. Potentiation of antitumor effect of cyclophosphamide and hydrazine sulfate by treatment with the antidiabetic agent, 1-phenylethylbiguanide (phenformin). *Cancer Letters* 7 (6):357-361.
- [23]Ma, J., Chen D., Lu K., Wang L., Han X., Zhao Y., Gong P. 2014. Design, synthesis, and structure–activity relationships of novel benzothiazole derivatives bearing the ortho-hydroxy N-carbamoylhydrazone moiety as potent antitumor agents. *European Journal of Medicinal Chemistry* 86 (0):257-269.
- [24]Dai, H., Xiao Y.-S., Li Z., Xu X.-Y., Qian X.-H. 2014. The thiazolmethoxy modification on pyrazole oximes: Synthesis and insecticidal biological evaluation beyond acaricidal activity. *Chinese Chemical Letters* 25 (7):1014-1016.
- [25]Ramadan M.El-Bahnasawy1 , F. A. E.-S., EimanH.A.Gaafer 1, Mohammed A.Wahba 2013. Benzilbisisonicotinoylhydrazone complexes of tervalent metals Ti, Zr, Sn, Hf and Th. *ICAIJ* 8 ((1)):1-6.
- [26]Archer, C. M., Dilworth J. R., Jobanputra P., Thompson R. M., McPartlin M., Povey D. C., Smith G. W., Kelly J. D. 1990. Development of new technetium cores containing technetium—nitrogen multiple bonds. Synthesis and characterization of some diazenido-, hydrazido- and imido- complexes of technetium. *Polyhedron* 9 (12):1497-1502.
- [27]Carrillo, D. 2000. [MoO<sub>2</sub>(acac)<sub>2</sub>], a versatile precursor for diazenido- and hydrazido-complexes. *Comptes Rendus de l'Académie des Sciences - Series IIC - Chemistry* 3 (3):175-181.
- [28]Riveros, P. C., Perilla I. C., Poveda A., Keller H. J., Pritzkow H. 2000. Tris(dialkyldithiocarbamate)diazenido(1-) and hydrazido(2-) molybdenum complexes: synthesis and reactivity in acid medium. *Polyhedron* 19 (22–23):2327-2335.
- [29]Svehla, G. (1979) Vogel's Textbook of macro and semimicro qualitative inorganic analysis. Longman London,
- [30]Welcher, F. J. 1958. analytical uses of ethylenediaminetetraacetic acid.



- [31] Vogel, A.A Text Book of Quantitative Inorganic Analysis, 1978. ELBS, London:474.
- [32] Figgis, B., Lewis J., Wilkins R. 1960. Modern coordination chemistry. Interscience, New York:403.
- [33] El-Tabl, A. S., El-Enein S. A. 2004. Reactivity of the new potentially binucleating ligand, 2-(acetichydrazido-N-methylidene- $\alpha$ -naphthol)-benzothiazol, towards manganese (II), nickel (II), cobalt (II), copper (II) and zinc (II) salts. *Journal of Coordination Chemistry* 57 (4):281-294.
- [34] Nicodemo, A., Araujo M., Ruiz A., Gales A. 2004. In vitro susceptibility of *Stenotrophomonas maltophilia* isolates: comparison of disc diffusion, Etest and agar dilution methods. *Journal of Antimicrobial Chemotherapy* 53 (4):604-608.
- [35] Standards, N. C. f. C. L. (2001) Performance standards for antimicrobial disk and dilution susceptibility tests for bacteria isolated from animals. Approved standard. Approved standard., vol M31-A2. NCCLS, Wayne, Pennsylvania
- [36] J.G. Collee, J.P. Duguid, A.G. Farser, B.D. Marmion e. (eds) (1989) *Practical medical microbiolog.* Churchill Livingstone., New York,
- [37] Gup, R., Kırkan B. 2005. Synthesis and spectroscopic studies of copper (II) and nickel (II) complexes containing hydrazone ligands and heterocyclic coligand. *Spectrochimica Acta Part A: Molecular and Biomolecular Spectroscopy* 62 (4):1188-1195.
- [38] El-Tabl, A. S., Shakhdofo M. M., El-Seidy A. M., Al-Hakimi A. N. 2012. Synthesis, characterization and antifungal activity of metal complexes of 2-(5-((2-chlorophenyl) diazenyl)-2-hydroxybenzylidene) hydrazinecarbothioamide. *Phosphorus, Sulfur, and Silicon and the Related Elements* 187 (11):1312-1323.
- [39] Raman, N., Muthuraj V., Ravichandran S., Kulandaisamy A. 2003. Synthesis, characterisation and electrochemical behaviour of Cu (II), Co (II), Ni (II) and Zn (II) complexes derived from acetylacetonandp-anisidine and their antimicrobial activity. *Journal of Chemical sciences* 115 (3):161-167.
- [40] Mendíl, D., Bílgín A., Gök Y., Şentük H. B. 2002. Synthesis and characterization of a new (E, E)-dioxime and its homo and heteronuclear complexes containing macrobicyclic moieties. *Journal of inclusion phenomena and macrocyclic chemistry* 43 (3-4):265-270.
- [41] Tircsó, G., Béneyei A., Brücher E., Kis A., Király R. 2006. Equilibria and structure of the lanthanide (III)-2-hydroxy-1, 3-diaminopropane-N, N, N', N'-tetraacetate complexes: Formation of alkoxo-bridged dimers in solid state and solution. *Inorganic chemistry* 45 (13):4951-4962.
- [42] Geraldes, C. F., Marques M. P. M., Sherry A. D. 1998. NMR conformational study of diamagnetic complexes of some triazatriacetate macrocycles. *Inorganic chimica acta* 273 (1):288-298.
- [43] Caminiti, R., Cucca P., Monduzzi M., Saba G., Crisponi G. 1984. Divalent metal-acetate complexes in concentrated aqueous solutions. An x-ray diffraction and NMR spectroscopy study. *The Journal of chemical physics* 81 (1):543-551.
- [44] Daumann, L. J., Schenk G., Ollis D. L., Gahan L. R. 2014. Spectroscopic and mechanistic studies of dinuclear metalohydrolases and their biomimetic complexes. *Dalton Transactions* 43 (3):910-928.
- [45] Deveci, P., Taner B., Kılıç Z., Solak A. O., Arslan U., Özcan E. 2011. Novel redox-active macrocyclic vic-dioxime ligand and its metal complexes modified with azacrown ether: Spectral, cyclic voltammetric and antimicrobial activity studies. *Polyhedron* 30:1726-1731.
- [46] Pavia, D., Lampman G., Kriz G., Vyvyan J. 2009. *Introduction to Spectroscopy* Cengage Learning. Belmont, CA, USA.
- [47] Naskar, S., Naskar S., Mondal S., Majhi P. K., Drew M. G., Chattopadhyay S. K. 2011. Synthesis and spectroscopic properties of cobalt (III) complexes of some aroylhydrazones: X-ray crystal structures of one cobalt (III) complex and two aroylhydrazone ligands. *Inorganic chimica acta* 371 (1):100-106.
- [48] Gulaczyk, I., Kręglewski M. 2008. The symmetric amino-wagging band of hydrazine: Assignment and analysis. *Journal of Molecular Spectroscopy* 249 (2):73-77.
- [49] Gulaczyk, I., Kręglewski M., Valentin A. 2003. The N-N stretching band of hydrazine. *Journal of Molecular Spectroscopy* 220 (1):132-136.
- [50] Singh G, Singh P, Singh K, Singh D, Handa R, Dubey N 2002. *Proc Natl Acad Sci Ind* 72A:87.
- [51] Monfared, H. H., Kalantari Z., Kamyabi M. A., Janiak C. 2007. Synthesis, Structural Characterization and Electrochemical Studies of a Nicotinamide-bridged Dinuclear Copper Complex derived from a Tridentate Hydrazone Schiff Base Ligand. *Zeitschrift für anorganische und allgemeine Chemie* 633 (11-12):1945-1948.
- [52] Pouralimardan, O., Chamayou A.-C., Janiak C., Hosseini-Monfared H. 2007. Hydrazone Schiff base-manganese (II) complexes: Synthesis, crystal structure and catalytic reactivity. *Inorganica Chimica Acta* 360 (5):1599-1608.
- [53] Kannan, S., Ramesh R. 2006. Synthesis, characterization, catalytic oxidation and biological activity of ruthenium (III) Schiff base complexes derived from 3-acetyl-6-methyl-2H-pyran-2, 4 (3H)-dione. *Polyhedron* 25 (16):3095-3103.
- [54] Lin-Vien, D., Colthup N. B., Fateley W. G., Grasselli J. G. (1991) *The handbook of infrared and Raman characteristic frequencies of organic molecules.* Elsevier,



- [55] El-Tabl, A. S., Plass W., Buchholz A., Shakdofa M. M. 2009. Synthesis, spectroscopic investigation and biological activity of metal (II) complexes with N<sub>2</sub>O<sub>4</sub> ligands. *Journal of Chemical Research* 2009 (9):582-587.
- [56] Kesioğlu, E., Gündüzalp A. B., Cete S., Hamurcu F., Erk B. 2008. Cr (III), Fe (III) and Co (III) complexes of tetradentate (ONNO) Schiff base ligands: synthesis, characterization, properties and biological activity. *Spectrochimica Acta Part A: Molecular and Biomolecular Spectroscopy* 70 (3):634-640.
- [57] Teotia, M., Gurtu J., Rana V. 1980. Dimeric 5- and 6-coordinate complexes of tri and tetradentate ligands. *Journal of Inorganic and Nuclear Chemistry* 42 (6):821-831.
- [58] Fouda, M., Abd-Elzaher M., Shakdofa M., El Saied F., Ayad M., El Tabl A. 2008. Synthesis and characterization of transition metal complexes of N'-[(1, 5-dimethyl-3-oxo-2-phenyl-2, 3-dihydro-1H-pyrazol-4-yl) methylene] thiophene-2-carbohydrazide. *Transition Metal Chemistry* 33 (2):219-228.
- [59] Nakamoto, K. (1978) *Infrared and Raman spectra of inorganic and coordination compounds*. Wiley Online Library,
- [60] Murukan, B., Mohanan K. 2006. Synthesis, Characterization, Electrochemical Properties and Antibacterial Activity of Some Transition Metal Complexes with [(2-hydroxy-1-naphthaldehyde)-3-isatin]-bishydrazone. *Transition Metal Chemistry* 31 (4):441-446.
- [61] El-Tabl, A. S., El-Saied F. A., Al-Hakimi A. N. 2007. Synthesis, spectroscopic investigation and biological activity of metal complexes with ONO trifunctionalized hydrazone ligand. *Transition Metal Chemistry* 32 (6):689-701.
- [62] K. N. (1967) *Infrared spectra of inorganic and coordination compounds* 2nd edn, Wiley Inc., New York
- [63] Steed, J. W., Tocher D. A. 1994. Nitrate complexes of ruthenium (IV): chelating, "semi-chelating" and monodentate coordination modes. *Polyhedron* 13 (2):167-173.
- [64] Nakamoto, K. (1986) *Infrared and Raman spectra of inorganic and coordination compounds*. Wiley Online Library,
- [65] Fouda, M. F., Abd-Elzaher M. M., Shakdofa M. M., El-Saied F. A., Ayad M. I., El Tabl A. S. 2008. Synthesis and characterization of a hydrazone ligand containing antipyrine and its transition metal complexes. *Journal of Coordination Chemistry* 61 (12):1983-1996.
- [66] Lever, A. 1968. Electronic spectra of some transition metal complexes: Derivation of D<sub>q</sub> and B. *Journal of Chemical Education* 45 (11):711.
- [67] Aslan, H. G., Özcan S., Karacan N. 2011. Synthesis, characterization and antimicrobial activity of salicylaldehydebenzenesulfonylhydrazone (<i>Hsalbsmh</i>) and its Nickel (II), Palladium (II), Platinum (II), Copper (II), Cobalt (II) complexes. *Inorganic Chemistry Communications* 14 (9):1550-1553.
- [68] Mohamed, G. G., Omar M., Hindy A. M. 2005. Synthesis, characterization and biological activity of some transition metals with Schiff base derived from 2-thiophene carboxaldehyde and aminobenzoic acid. *Spectrochimica Acta Part A: Molecular and Biomolecular Spectroscopy* 62 (4):1140-1150.
- [69] Geary, W. J. 1971. The use of conductivity measurements in organic solvents for the characterisation of coordination compounds. *Coordination Chemistry Reviews* 7 (1):81-122.
- [70] Chohan, Z. H., Supuran C. T. 2005. Organometallic compounds with biologically active molecules: in vitro antibacterial and antifungal activity of some 1, 1'-(dicarbohydrazono) ferrocenes and their cobalt (II), copper (II), nickel (II) and zinc (II) complexes. *Applied organometallic chemistry* 19 (12):1207-1214.
- [71] Akbar Ali, M., Mirza A. H., Yee C. Y., Rahgeni H., Bernhardt P. V. 2011. Mixed-ligand ternary complexes of potentially pentadentate but functionally tridentate Schiff base chelates. *Polyhedron* 30 (3):542-548.
- [72] Surati, K. R., Thaker B. 2010. Synthesis, spectral, crystallography and thermal investigations of novel Schiff base complexes of manganese (III) derived from heterocyclic β-diketone with aromatic and aliphatic diamine. *Spectrochimica Acta Part A: Molecular and Biomolecular Spectroscopy* 75 (1):235-242.
- [73] Surati, K. R. 2011. Synthesis, spectroscopy and biological investigations of manganese (III) Schiff base complexes derived from heterocyclic β-diketone with various primary amine and 2, 2'-bipyridyl. *Spectrochimica Acta Part A: Molecular and Biomolecular Spectroscopy* 79 (1):272-277.
- [74] Kennedy, B. J., Murray K. S. 1985. Magnetic properties and zero-field splitting in high-spin manganese (III) complexes. 1. Mononuclear and polynuclear Schiff-base chelates. *Inorganic Chemistry* 24 (10):1552-1557.
- [75] Hathaway, B. J., Billing D. E. 1970. The electronic properties and stereochemistry of mono-nuclear complexes of the copper(II) ion. *Coordination Chemistry Reviews* 5 (2):143-207.
- [76] Eisenstein, J. C. 1958. Effect of Exchange Interaction on the Magnetic and Thermal Properties of Copper Salts and Copper Coordination Compounds. *The Journal of Chemical Physics* 28 (2):323-329.
- [77] Tomlinson, A. A. G., Hathaway B. J. 1968. The electronic properties and stereochemistry of the copper(II) ion. Part II. The monoamine adducts of bisethylenediaminecopper(II) complexes. *Journal of the Chemical Society A: Inorganic, Physical, Theoretical* (0):1685-1688.



- [78]El-Tabl, A. S., Aly F. A., Shakdofa M. M. E., Shakdofa A. M. E. 2010. Synthesis, characterization, and biological activity of metal complexes of azohydrazone ligand. *Journal of Coordination Chemistry* 63 (4):700-712.
- [79]Al-Hakimi, A. N., El-Tabl A. S., Shakdofa M. M. 2009. Coordination and biological behaviour of 2-(p-toluidino)-N'-(3-oxo-1, 3-diphenylpropylidene) acetohydrazone and its metal complexes. *Journal of Chemical Research* 2009 (12).
- [80]Shauib, N. M., Elassar A.-Z. A., El-Dissouky A. 2006. Synthesis and spectroscopic characterization of copper (II) complexes with the polydentate chelating ligand 4, 4'-[1, 4-phenylenedi (nitriolo) dipente-2-one. *Spectrochimica Acta Part A: Molecular and Biomolecular Spectroscopy* 63 (3):714-722.
- [81]Greenwood, N. N., Straughan B. P., Wilson A. E. 1968. Behaviour of tellurium(IV) chloride, bromide, and iodide in organic solvents and the structures of the species present. *Journal of the Chemical Society A: Inorganic, Physical, Theoretical* (0):2209-2212.
- [82]Symons, M. C., Trousson P. M. 1984. Electron spin resonance studies of the radiolysis of methyl isocyanate and methyl isothiocyanate. *Radiation Physics and Chemistry* (1977) 23 (1):127-135.
- [83]A. S. Eltabl, M. M. A.-E. W., M. A. Wahba, S. A. EL-assaly, L. M. Saad 2014. Sugar Hydrazone Complexes; Synthesis, Spectroscopic Characterization and Antitumor Activity. *Journal of Advances in Chemistry* 9 (1):1837-1860.
- [84]Feng, G., Mareque-Rivas J. C., Williams N. H. 2006. Comparing a mononuclear Zn (II) complex with hydrogen bond donors with a dinuclear Zn (II) complex for catalysing phosphate ester cleavage. *Chemical Communications* (17):1845-1847.
- [85]Mareque-Rivas, J. C., Prabakaran R., Parsons S. 2004. Quantifying the relative contribution of hydrogen bonding and hydrophobic environments, and coordinating groups, in the zinc (II)-water acidity by synthetic modelling chemistry. *Dalton transactions* (10):1648-1655.
- [86]Tweedy, B. Possible mechanism for reduction of elemental sulfur by moniliniafructicola. In: *Phytopathology*, 1964. AMER PHYTOPATHOLOGICAL SOC 3340 PILOT KNOB ROAD, ST PAUL, MN 55121, pp 910-&
- [87]Chohan, Z. H., Khan K. M., Supuran C. T. 2005. In-vitro antibacterial, antifungal and cytotoxic properties of sulfonamide-derived Schiff's bases and their metal complexes. *Journal of enzyme inhibition and medicinal chemistry* 20 (2):183-188.
- [88]Al-Hakimi, A. N., El-Tabl A. S., Shakdofa M. M. 2009. Coordination and biological behaviour of 2-(p-toluidino)-N'-(3-oxo-1, 3-diphenylpropylidene) acetohydrazone and its metal complexes. *Journal of Chemical Research* 2009 (12):770-774.